UNITED NATIONS UNIVERSITY
GEOTHERMAL TRAINING PROGRAMME
Orkustofnun, Grensasvegur 9,
IS-108 Reykjavik, Iceland

Reports 2012
Number 15

UPDATED RESERVOIR ANALYSIS OF THE THEISTAREYKIR HIGH-TEMPERATURE GEOTHERMAL FIELD, N-ICELAND

Shakiru Idrissa Kajugus
Tanzania Electric Supply Company Ltd. – TANESCO
Research Department
P.O. Box 9024, Dar es Salaam
TANZANIA
shakiru.idrissa@tanesco.co.tz; shakiru_idrissa@yahoo.co.uk

ABSTRACT

Theistareykir high-temperature geothermal field is located in the Theistareykir fissure swarm in Thingeyjarsýsla region, about 32 km from the coast in northeast Iceland. The bedrock in the area is divided into basaltic hyaloclastites from subglacial eruptions during the Ice Age, interglacial lava flows and recent lava flows (aged about 10,000 years and younger). A surface resistivity survey shows that at a depth of 800-1000 m the Theistareykir geothermal system covers an area of 45 km^2 surrounded by a low-resistivity cap which is underlain by a high-resistivity core. To date, eight deep wells have been drilled in the area, three vertical and five directional wells. The up-flow zone is located where well THG-1 was drilled and extends in a northeast direction. Temperature below 1500 m b.s.l. is above 300°C on the eastern side (where wells THG-1, THG-4, THG-6 and THG-7 are located) of the reservoir spreading in a northeast direction. THG-8 turned out to be a cold well and its formation temperature is less than 170°C below 800 m b.s.l. Generally the Theistareykir area is characterized by a cold inflow at a shallow depth. Injection well test analyses done for wells THG-7 and THG-8 show that the model that best fits the data is of a homogenous reservoir with constant boundary pressure. Skin factor values indicate that the wells are in good contact with the reservoir, which may be due to the stimulation of the wells done after completion. Generally both wells are characterised by good permeability as well as storativity. Volumetric assessment using Monte Carlo calculations estimated that about 160 MWe could be generated for a production period of 30 years and 90 MWe if the production time was extended to 50 years.

1. INTRODUCTION

Theistareykir high-temperature geothermal field is located in the Theistareykir fissure swarm in Thingeyjarsýsla region about 32 km from the coast in Northeast Iceland. The location of the project area is shown in Figure 1. It was a well-known geothermal field for many centuries as the main sulphur mine in Iceland, providing the Danish king with raw material for gun powder. Thermal activity is easily observed when looking at the landscape and surface manifestations. The first geothermal exploration was carried out in 1972-1974 (Grönvold and Karlsdóttir, 1975), and a major geothermal assessment was made in 1981-1984 (Layugan, 1981; Gíslason et al., 1984; Ármannsson et al., 1986; Darling and

FIGURE 1: Map showing location of Theistareykir high-temperature geothermal field (obtained from Google Earth, 2012)

Ármannsson, 1989). In 1991-2000 the area was monitored periodically (Ármannsson et al., 2000). A previous study by Ármannsson et al. (1986) showed that the geothermal activity covers an area of about 10.5 km^2, and the intensity is greatest on the northwest slopes of Mt. Baejarfjall and in the pasture extending from the northern to the western part of Mt. Ketilfjall (Figure 2). If the old alteration in the western part of the swarm is considered to be a part of the thermal area, then it covers approximately 20 km^2 (Figure 2). However, the geophysical studies conducted by ISOR in the years 2004 and 2006 in the area revealed that at a depth of 800-1000 m the high-resistivity core of the Theistareykir geothermal system covered an area of 45 km^2, surrounded by a low-resistivity cap (Figure 4); but this is the deeper limit for TEM measurement penetration (Karlsdóttir et al., 2006).

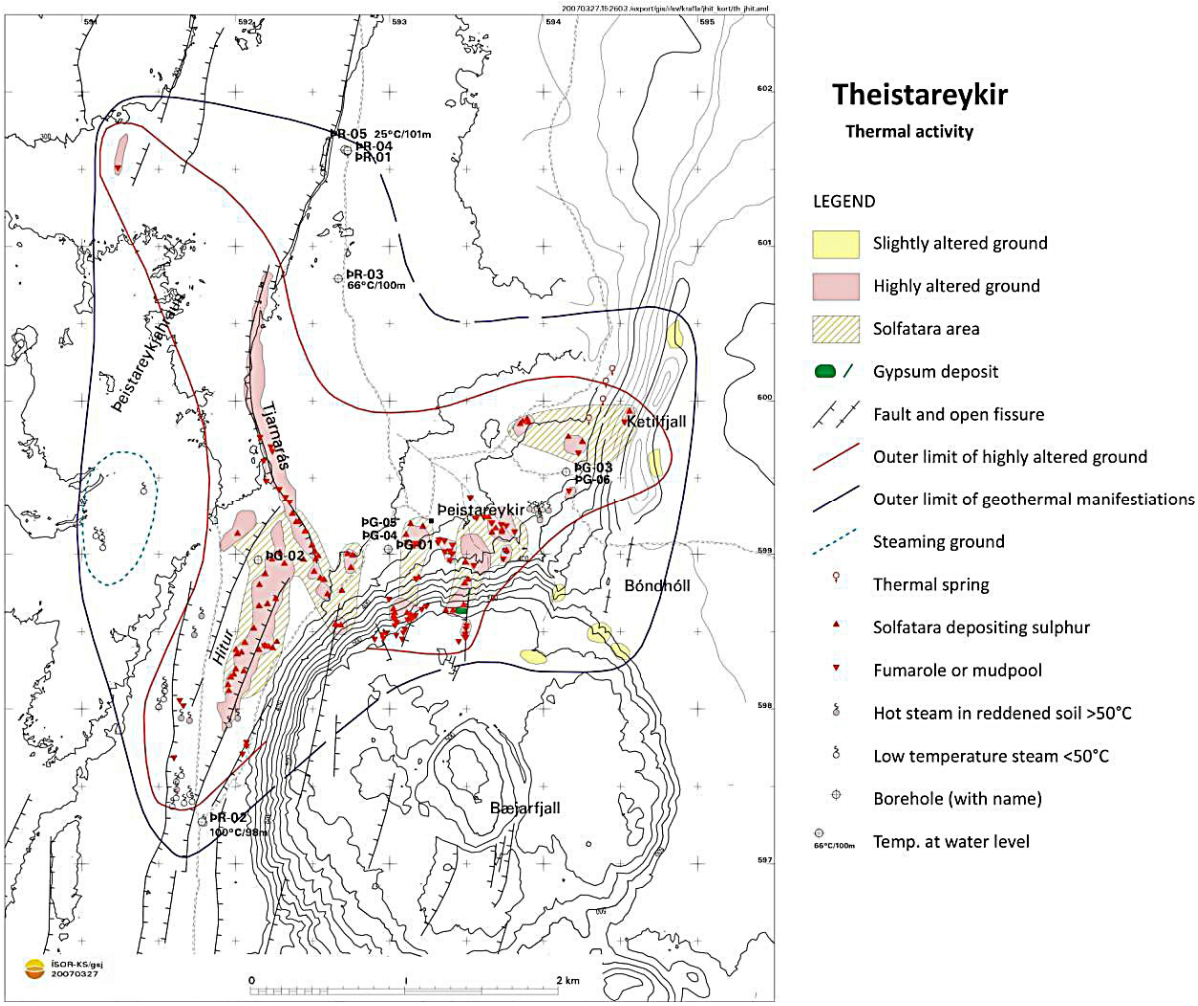

FIGURE 2: Geothermal map of the Theistareykir high-temperature field (Ármannsson, 2011)

Ármannsson et al. (1986) divided the active surface area into five sub-areas (Figure 3), three of which (A, C and D) appeared promising for drilling. Exploratory drilling in the area started in 2002 by the company Theistareykir Ltd. Since then, eight deep exploration wells have been drilled in the area. In 2008, a detailed conceptual model of the area was developed based on recent data from the exploration wells as well as on the previous studies mentioned above (Gudmundsson et al., 2008).

As part of the 2008 study by Gudmundsson et al., a volumetric assessment was preformed based on the conceptual model. A more detailed reservoir model was then developed using the TOUGH2 code (Arnaldsson et al., 2011). The main results of the volumetric assessment in 2008 were that the system could sustain 100-150 MWe production for 100 years. The volumetric assessment results covered a very wide range, mainly due to uncertainty in the surface area of the region and the recovery factor. The uncertainty was expected to decrease with further drilling. The main results of the numerical model in 2011 were that the system could sustain 100 MWe power production for 30 years.

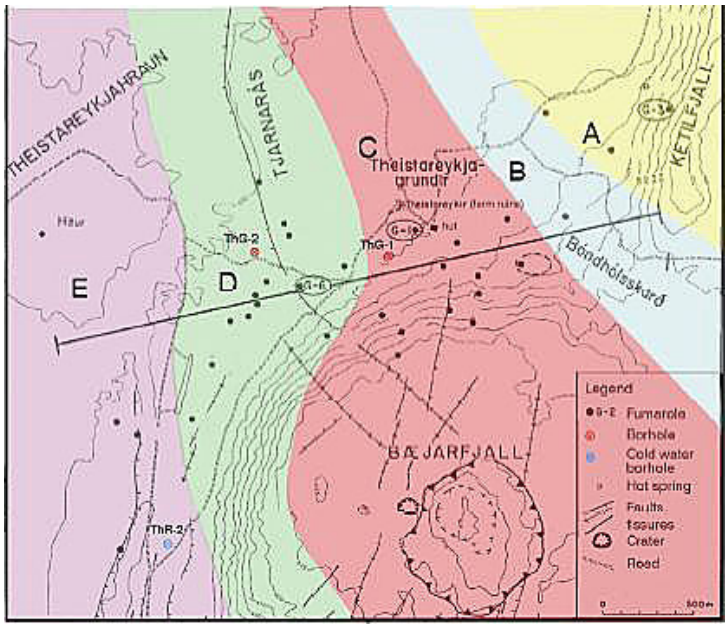

FIGURE 3: Division into five sub-areas in Theistareykir (Darling and Ármannsson, 1989)

The purpose of this project is to update the previous analyses on the initial conditions of the reservoir, which are the initial pressure and formation temperature, in addition to reservoir parameters inferred from well testing, i.e. the transmissivity, storativity and discharge characteristics of the wells. Finally, a reassessment by the volumetric method will be conducted to estimate and refine the potential of the geothermal system within the Theistareykir high-temperature field.

2. GEOTHERMAL EXPLORATION

2.1 Geological exploration

The bedrock in the area is divided into basaltic hyaloclastites resulting from subglacial eruptions during the Ice Age, interglacial lava flows and recent lava flows (aged about 10,000 years and younger). Acidic rocks are found on the western side of the fissure swarm, from subglacial eruptions up to the last glacial period. Rifting is still active in the fissure swarm and faults and fractures have opened in recent times.

Volcanic activity has been relatively infrequent in the area in recent times. Approximately 14 volcanic eruptions have occurred in the last 10,000 years, but none in the last 2500 years. Large earthquakes (up to M7) occur mainly north of the area in the Tjörnes Fracture Zone, which is a right-lateral transform fault. They also occur in the fissure swarm itself during rifting. The Tjörnes Fracture Zone strikes northwest, crosscutting the north-striking fractures as it enters into the fissure swarm some 5 km north of the thermal area. The volcanic activity ceases in the fissure swarm as it crosses the Tjörnes Fracture Zone, although its northern part remains seismically active. The most active parts of the area are related to active fractures, which increase permeability and enable geothermal fluids to circulate and reach the surface (Ármannsson et al., 1986).

2.2 Geophysical exploration

In the years 2004 and 2006 ISOR conducted an electrical resistivity survey at Theistareykir high-temperature geothermal field (Karlsdóttir et al., 2006) employing the TEM method, which is limited to shallow depths of around 800-1000 m. The report suggested that the MT method should be conducted in the area to resolve the resistivity at a greater depth than the previous TEM measurements. In 2007, KMS Technologies in cooperation with VGK Hönnun, presently Mannvit, conducted an MT survey at Theistareykir for Theistareykir Ltd. (KMS Technologies, 2008). In 2009, further studies followed and additional MT and TEM measurements were conducted by ISOR. The following are the results presented by Karlsdóttir and Vilhjálmsson (2011) in their report.

- The TEM measurements revealed that at a depth of 800-1000 m, the Theistareykir high-temperature geothermal system covers an area of 45 km^2 surrounded by a low-resistivity cap (Figure 4) which is underlain by a high-resistivity core.
- The MT measurements show a deeper seated low-resistivity layer beneath the entire survey area with a centre at nearly 15 km depth below the surface in the southern part of the area. Below Theistareykir and in the northern part of the survey area, the centre is considerably shallower, or at a depth of 8 km beneath the surface.

2.3 Wells

The extensive surface exploration of the field, which appeared to be promising, led to the initiation of the next step of exploration, deep exploration drilling, to obtain subsurface information about the field. The drilling started in 2002 by Theistareykir Ltd. Prior to drilling deep wells, a number of shallow wells (100-200 m depth) were drilled to survey groundwater patterns and to obtain a suitable source of cold water during drilling of the deep exploration wells. At present, eight deep exploration wells have been drilled in the area. In this project report, the temperature and pressure data from the warm-up measurements in six wells (THG-1, THG-2, THG-4, THG-6, THG-7 and THG-8) have been analysed and interpreted. In addition, an interpretation was carried out on the results of tests for two wells (THG-7 and THG-8). This project paper is aimed at updating the previous reservoir analysis of the field and will, therefore, only present the formation temperature and pressure analysis for three newly drilled wells (THG-6, THG-7 and THG-8).

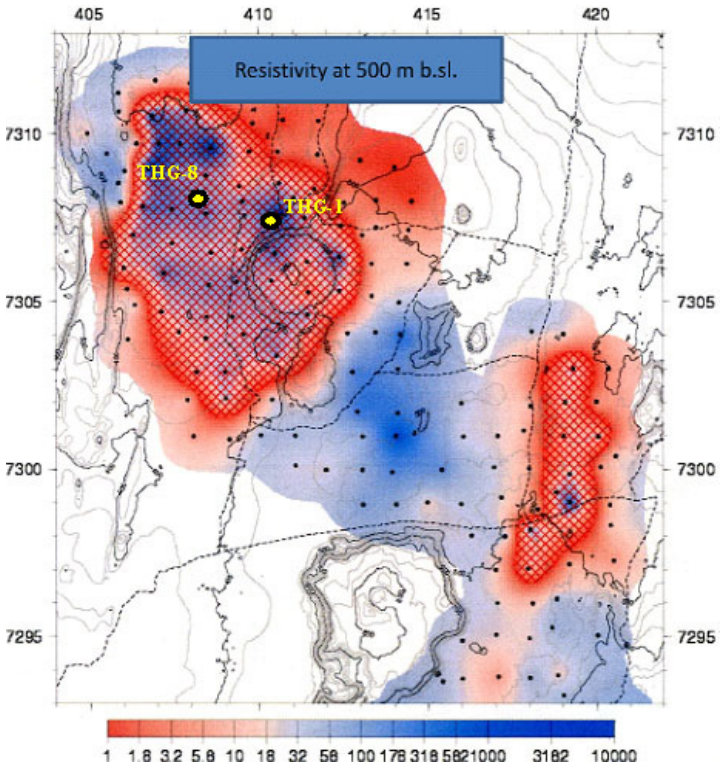

FIGURE 4: Resistivity at 500 m b.s.l. at Theistareykir according to the TEM survey 2004–2006 (Karlsdóttir et al., 2006)

Well THG-1 was the first deep well to be drilled in the area in 2002. It is located in area C (Figures 3 and 5) and was drilled to a depth of 1953.2 m. This is a vertical well with a casing depth of 609.5 m. Well THG-2 is a vertical well drilled in the year 2003 on the western side of well THG-1 to a depth of 1723 m and cased to a depth of 611.1 m. In 2006, well THG-3 followed, also a vertical well drilled to

the northeast of well THG-1. The final depth for well THG-3 was 2659 m and it has a casing depth of 757 m. THG-4 and THG-5 are both directional wells drilled in the year 2007 from the same platform as well THG-1. THG-4 is directed to the southeast beneath Mt. Baejarfjall and was drilled to a depth of 2239.5 m and cased to a depth of 824.7 m. THG-5 is diverted towards THG-2, has a final depth 1909.7 m and is cased to a depth of 847 m. In 2008, well THG-5B was drilled as a side track from well THG-5 with a small angle in the same direction. Wells THG-6 and THG-7 were drilled directionally in 2008 and 2011, respectively, from the same platform as THG-3. THG-6 is directed to the northwest while THG-7 goes to the northeast. The final and casing depth of wells THG-6 and THG-7 are 2798.9 and 841 m, and 2509 and 776 m, respectively. Finally, in 2011, well THG-8 was drilled as a directional well about 1.5 km away from well THG-2 and trending to the northwest with a casing depth of 1493 m and the final depth reached was 2496 m. The location and summary of each well considered in this report in the Theistareykir high-temperature field are shown in Figure 5 and Table 1, respectively.

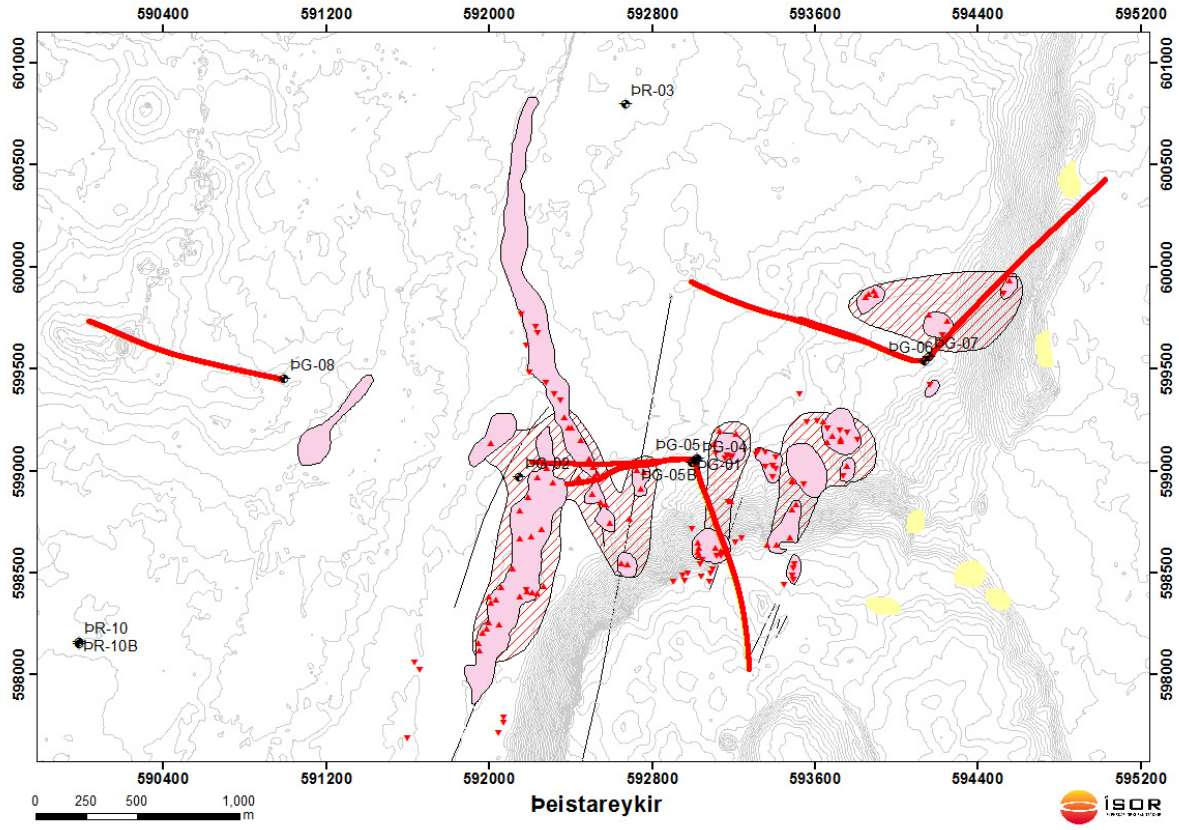

FIGURE 5: Map showing location of the wells and their directions (THG = ÞG)

TABLE 1: Summary of the wells in Theistareykir high-temperature field

Well	THG-1	THG-2	THG-4	THG-6	THG-7	THG-8
Year drilled	2002	2003	2007	2008	2011	2011
Type	Vertical	Vertical	Directional	Directional	Directional	Directional
Design drilling angle			35°	30°	35°	
Dir. of angle from well head			160°	285°	45°	
Well coordinates (x;y)	592920; 599033	592145; 598963	593013.96; 599041.77	594134.5; 59953.70	594154.5; 599552.2	596991.48; 599447.02
Casing depth (m)	609.5	611.1	824.7	846	776	1493
Elevation (m a.s.l.)	352	330	352	400	375	340
Measured depth (m)	1953.2	1723	2239.5	2798.9	2509	2496
True vertical depth (m)	1601.2	1393	1879.2	2473.86	2072.35	2236.94

3. ANALYSIS OF TEMPERATURE AND PRESSURE IN THEISTAREYKIR FIELD

3.1 Temperature and pressure profile interpretation

Temperature (T) and pressure (P) are essential parameters in a geothermal system. The information obtained from knowledge of these parameters is of great value in understanding different properties of the geothermal system, such as the physical state of the system, flow patterns, location of the aquifers/feed zones, thermal gradient heat flow and in managing the geothermal field.

The temperature and pressure in a geothermal system can be determined by various techniques and the most common is the measurement of the temperature in the drilled wells in the system. This is done by dipping down the logging tools to the bottom of the wells where data are recorded, after which the tools are retrieved back to the surface. The tools can be mechanical or electronic; nevertheless, data accuracy is most important. Temperature and pressure measurements are usually obtained during drilling (inside the drill string before pulling it out), after pulling the drill string out (still injecting cold water), during the warm-up period (no injection and closed well) and regular measurements for monitoring the state of the reservoir. However, it is a fact that the conditions in the wells during logging differ from that of an undisturbed geothermal system before drilling; this is a result of various effects that can disturb temperature and pressure.

The warm-up data from six wells (THG-1, THG-2, THG-4, THG-6, THG-7 and THG-8) in Theistareykir geothermal area were considered for interpretation in this project paper. The first three wells (THG-1, 2 and 4) were used to compare with the previous results obtained in this field. Moreover, they were used in creating the formation temperature and initial pressure plots as well as contour cross-sections (the plots of these three wells are presented in Appendix I). This report only presents the results and discusses in detail the wells that were drilled recently, which are THG-6, 7 and 8. These temperature and pressure data were plotted against measured depth to obtain the temperature and pressure profiles (Figures 6-8).

3.1.1 Well THG-6

Three temperature and pressure profiles were plotted against measured depth from the warm-up data (Figure 6). Three feed zones are located at a depth of around 850, 1050 and down to 2650 m. The main feed zones appear to be at a depth of 850 and 2650 m. The profiles from the top down to a depth similar

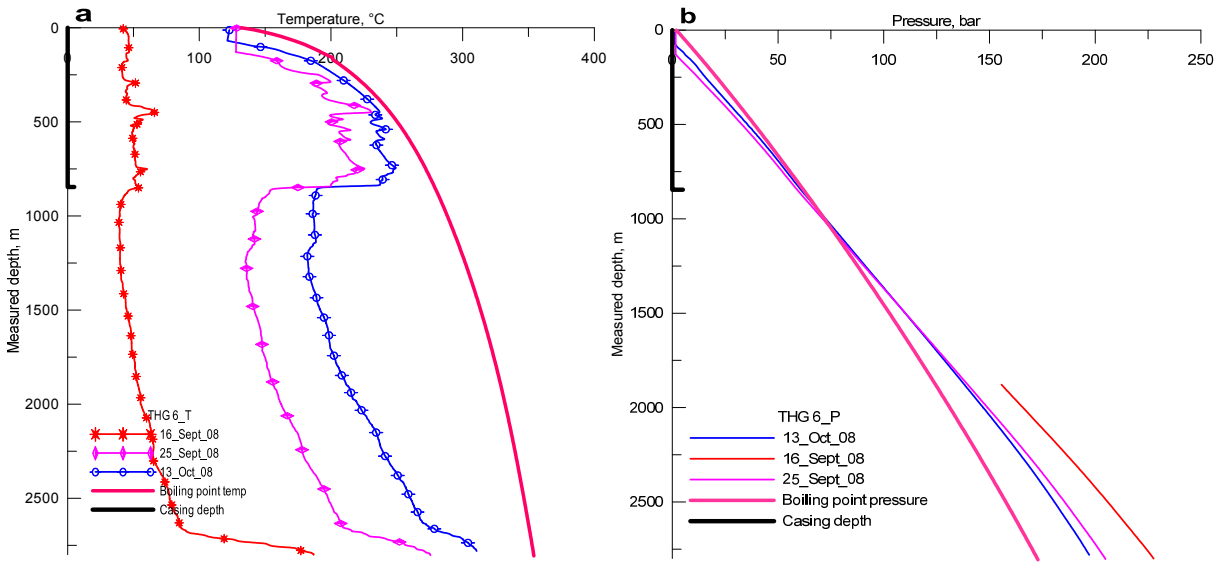

FIGURE 6: Temperature (a) and pressure (b) profiles for THG-6 from the warm-up data plotted on the measured depth alongside the boiling point curve

to that of the casing (0-850 m) behave as the boiling point curve, while a negative temperature gradient at a depth below the casing depth down to 1200 m was observed. Below that, an isothermal profile is visible from a depth of 1200 m down to the final depth. The isothermal condition could be due to water circulation from the aquifers at 850 and 1050 m.

The oscillations of the profiles at the casing depth indicate the water movements in that part of the reservoir at the eastern side of the field; this was observed in all the wells drilled in that part of the field and they all behave the same way at the interval of 0-800 m depth.

Figure 6b shows the pressure profiles from the warm-up data. The profiles indicate that the pivot point lies at a depth of 1400 m and the pressure is 107 bar at that point. The pivot point seems situated at the midpoint between the two main feed zones, which are at 850 and 2650 m.

3.1.2 Well THG-7

In Figure 7a are four temperature profiles from the warm-up data obtained from well THG-7. From the profiles, three feed zones can be observed. The first feed zone is at a depth of around 700 m, which is similar to that of the casing, the second feed zone is at 1400-1700 m and the last is at 2250 m. The profiles tend to behave in the same way as those from well THG-6. They follow the shape of the boiling point curve in the upper part of the well down to the end of the casing depth; then they reverse at 700 m and below that show isothermal behaviour down to the final drilled depth. In this well, the isothermal trend is rather near to the shape of the boiling temperature curve, which is disturbed in the third (2250 m) feed zone where there is colder inflow.

The reverse in temperature can be explained as in THG-6 because these two wells were drilled from the same platform as well as THG-3, which also shows the same behaviour. However, it is not only the wells that were drilled from the same platform which show this behaviour, but also the wells (THG-1 and THG-4) located in the eastern part of the field.

In the pressure profiles of this well, the pivot point was observed at a depth of 1250 m where the pressure is 106.5 bar (Figure 7b). This indicates an inter zone flow between the two aquifers (at 700 and 2250 m).

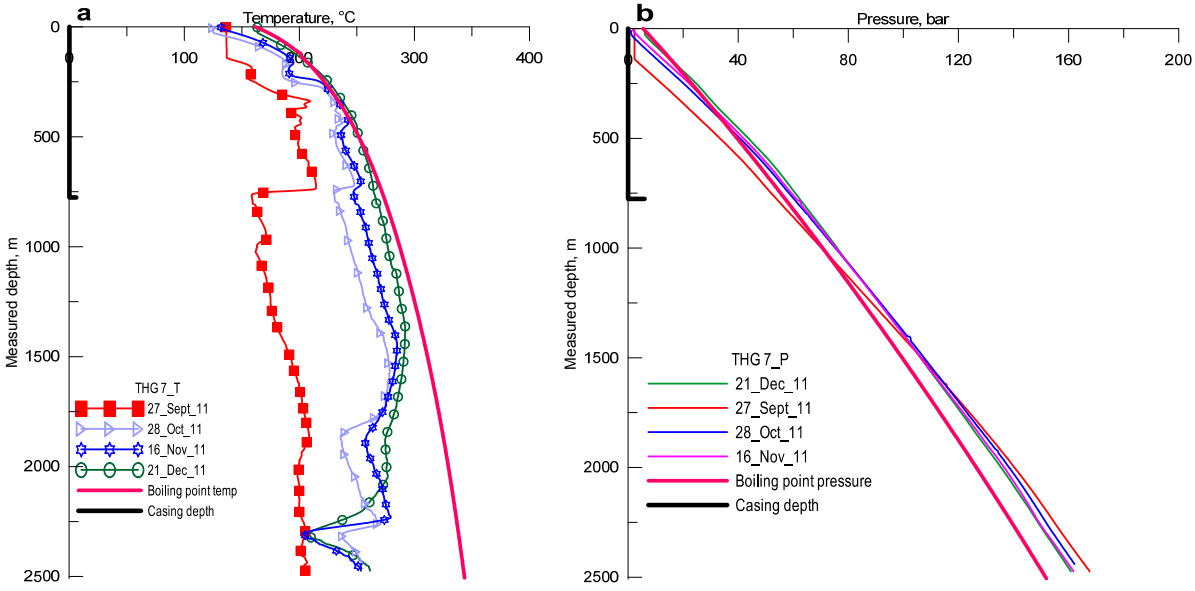

FIGURE 7: Temperature (a) and pressure (b) profiles for THG-7 from the warm-up data plotted on the measured depth alongside the boiling point curve

3.1.3 Well THG-8

Only two warm-up temperature measurements were available in this well and they were plotted against measured depth in order to interpret the feed zones and the temperature trending, as can be seen in Figure 8a. The feed zones are found at depths 980 – 1250 m, 1500 – 1700 m and 2100 m. In the upper part of the well inside the casing from depth 0 -500 m, the profiles show the conductive profile with the temperature increasing linearly with depth. Then cold inflow is observed at a depth of around 500 m and a reverse in temperature is observed from this depth down to the final depth. The other two aquifers (at 1500-1700 m and 2100m) circulate colder fluid and, together, contribute to the cooling of this well which turned out to be a cold well.

Figure 8b shows the two warm-up pressure profiles with the pivot point at a depth of 1960 m and the pressure of 152.5 bar at the pivot point.

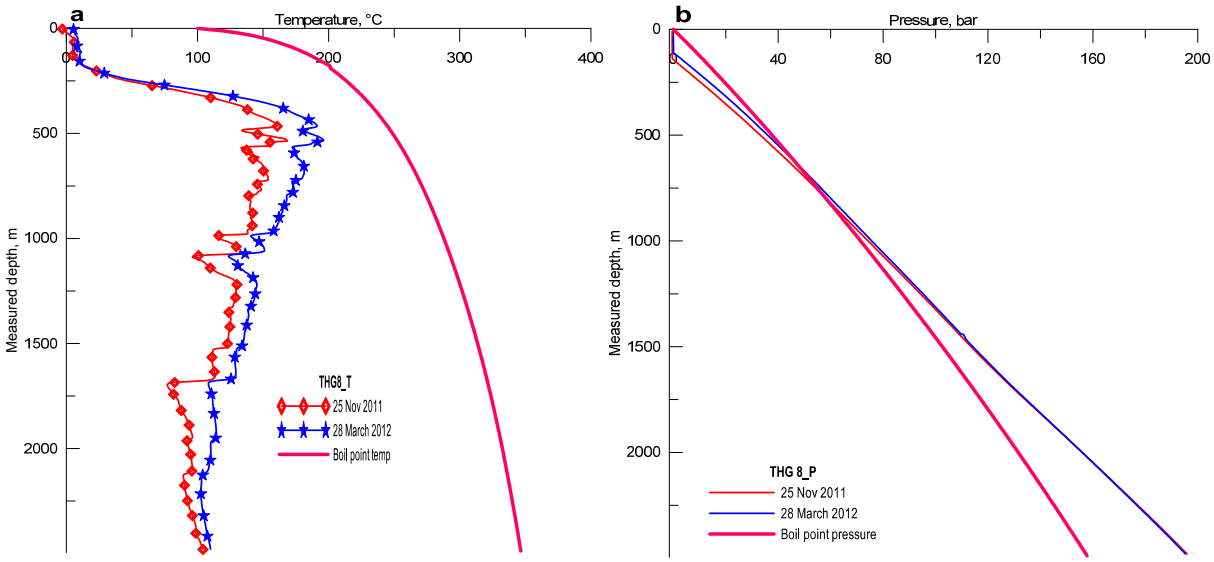

FIGURE 8: Temperature (a) and pressure (b) profiles for THG-8 from the warm up data plotted on the measured depth alongside the boiling point curve

Table 2 summarises all the pivot points of these three wells as well as for the other three wells from which the warm-up pressure profiles were interpreted.

TABLE 2: The pivot point of each well and their depth and pressure

Well	No. of pivot points	Depth to pivot point (TVD) (m)	Pressure at pivot point (bar)
THG-1	1	1130	88
THG-2	1	970	76.7
THG-4	1	1380	118
THG-6	1	1400	107
THG-7	1	1250	106.5
THG-8	1	1960	152.5

3.2 Estimation of formation temperature and initial pressure in the Theistareykir field

Formation temperatures are the equilibrium temperatures between geothermal fluid and rock in a geothermal system. The formation temperatures of geothermal wells help in deriving the conceptual

model of the system and are important in decision making during well completion. Estimation of the formation temperature and pressure is a process which involves several steps for determination.

Initially, the measured depth of every borehole was converted to true vertical depth and the temperature and pressure profiles were plotted against it. The boiling point curve was also plotted alongside the profiles on the same graph. The boiling point curves were calculated from the software *Boilcurv* found in the ICEBOX programme package developed by ÍSOR, and calculated the temperature and pressure with respect to depth by assuming the initial water level of every borehole as described in the ICEBOX user's manual (Arason et al., 2004). Again, software from the ICEBOX package known as *Berghiti* was used to estimate the formation temperature at certain selected depths. The software implements the Horner's plot and Albright methods to determine temperature from the historical warm-up data. The Albright method is mainly used to interpret temperature measurements during drilling. The Horner's plot method applies for longer data histories and was, therefore, used to analyse the estimation temperature. After obtaining the Horner's point at a certain depth, then the formation temperature curves of every borehole were plotted and compared with the original profiles, boiling point curve and Horner's points.

Predyp is another piece of software included in ICEBOX and calculates the initial pressure from a known temperature column and initial water level or wellhead pressure. The pressures from *Predyp* were plotted alongside the pressure profiles and the boiling point curve and the pivot points as well as the initial pressures that were obtained.

3.2.1 THG-6

The formation temperature in the upper part of the well down to the depth of the casing at 850 m falls on the boiling point curve, followed by a down-flow pattern to the final depth. The Horner's points were selected at the depth of the main feed zones (at 850, 1050 and 2650 m) and only the Horner's points estimated at the bottom were used; they all showed the same trend as the warm-up profiles (Figure 9a). This can be best explained by water flowing into the well from the upper aquifer at 850 m. As it flows down the well, it gains heat and approaches the boiling point curve. However, a reverse in temperature was encountered at a depth of around 850 m. Figure 9b shows a pressure pivot point reached at 1400 m depth, where the pressure is 107 bar. The pressure profiles follow the estimated formation pressure and the initial pressure at the wellhead is 2 bar.

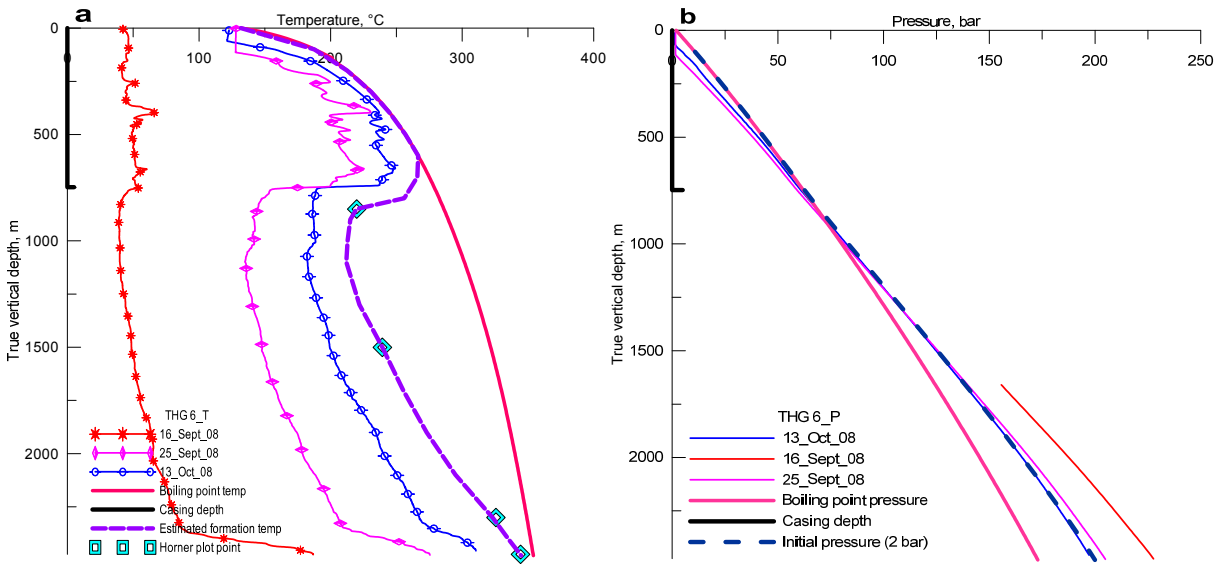

FIGURE 9: Warm-up temperature (a) and pressure profiles (b) plotted together with estimated formation and initial pressure, respectively, for well THG-6

3.2.2 THG-7

Figure 10a shows the formation temperature for THG-7, estimated using the boiling point curve. As can be observed from the temperature profiles in the upper part of the well, they fall on the boiling point curve, then follow a slight reverse in temperature at the middle and a small heat gain is observed down the well to the second aquifer, where there is a clear inflow of cooler water, indicated by the reverse in temperature. The Horner's plot points all fall onto the boiling point curve which helps to suggest that the formation temperature of this well is well represented by the boiling point curve.

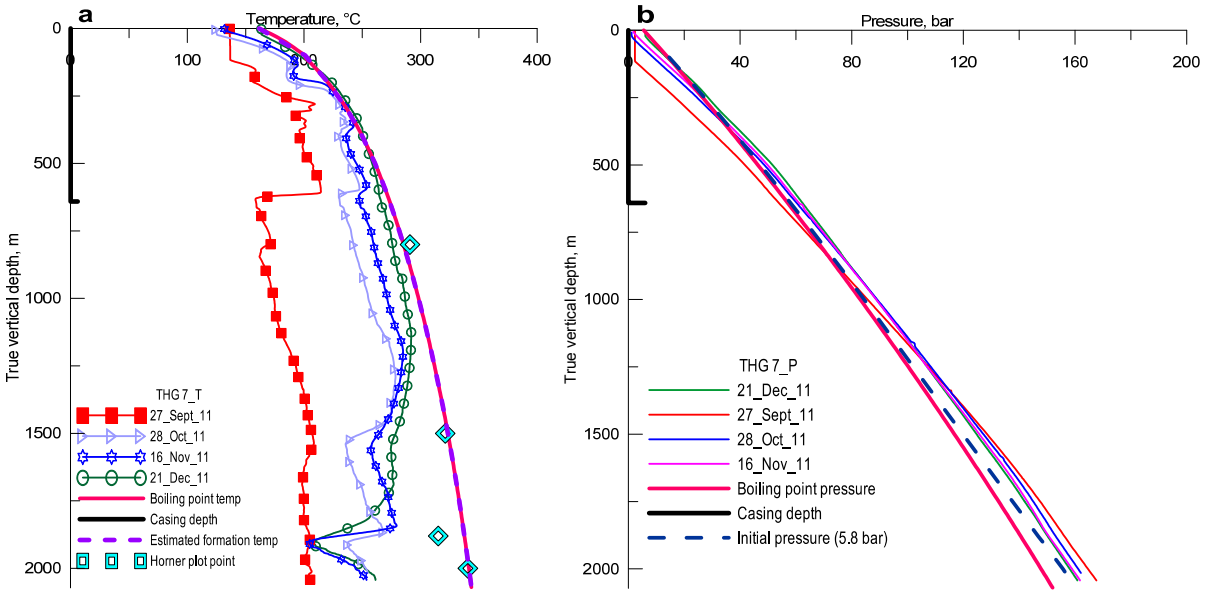

FIGURE 10: Warm-up temperature (a) and pressure profiles (b) plotted together with estimated formation and initial pressure, respectively, for well THG-7

3.2.3 THG-8

This is the well drilled on the western side of the Theistareykir area and which turned out to be cold all the way down to the final drilled depth. The formation temperature was interpreted from the only two warm-up profiles which were available. No Horner's points were plotted, since a minimum of 3 points are required to use the Horner method. At the upper part of the well there is cold inflow and heat is gained by conduction. An inversion of temperature appears at a depth of 500 m and is visible down to the final depth. It seems that the aquifers at 1500-1700 m and 2100m contribute cold inflow into the well; the heat is lost by convection. The formation temperature estimated at the bottom of the well is below 150°C (Figure 11a). The pivot point was observed at depth 1960 m and the pressure was 152.5 bar (Figure 11b).

3.3 Temperature and pressure maps and cross-sections

Based on the formation temperatures and initial pressures from the six wells THG-1, THG-2, THG-4, THG-6, THG-7 and THG-8, estimated as part of this study, two maps at 500 and 1500 m b.s.l. and two cross-sections with different directions (A-A' and C-C') were made so as to evaluate the temperature and pressure distribution in the field. The A-A' cross-section was drawn parallel to the East axis where all six wells are connected, while that of C-C' was drawn in a NE-SW direction, which cuts through THG-1, THG-2, THG-4, THG-6 and THG-7. This C-C' cross section was chosen based on maps which show that the temperature increase is trending in the same direction (NE-SW). Moreover, the section was drawn for comparison purposes with the previous cross-sections drawn with the same trend made

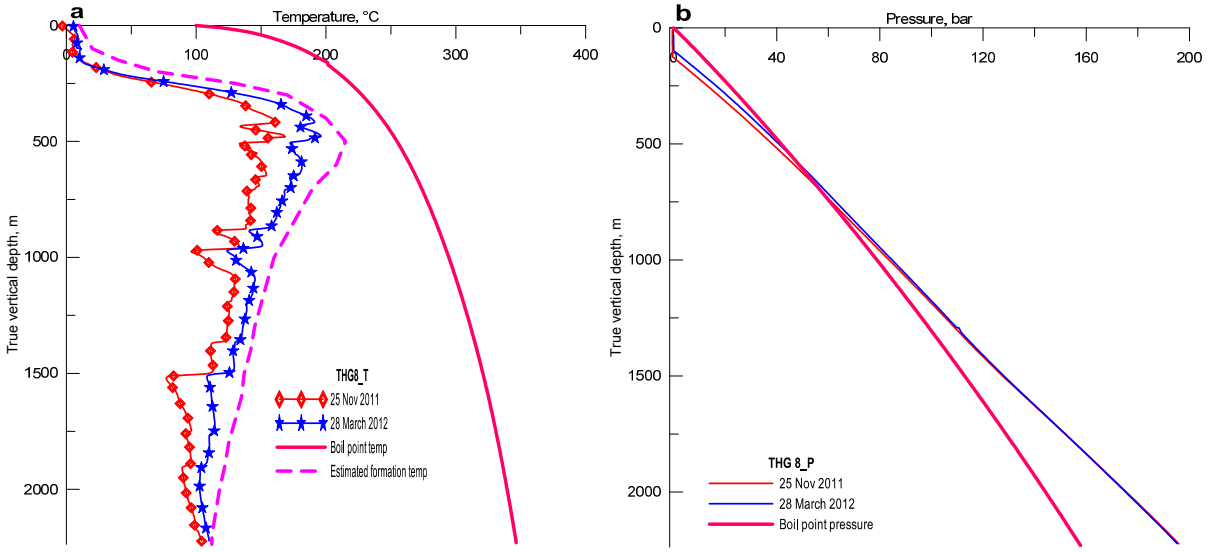

FIGURE 11: Warm-up temperature (a) and pressure profiles (b) plotted together with estimated formation and initial pressure, respectively, for well THG-8

by Gudmundsson et al. (2008). The formation temperatures and pressure values from the directional wells were projected to the vertical plane before plotting the vertical section.

Both maps and vertical cross-sections in Figures 12-15 show that the temperature increases in a northeast direction, which appears to be the location of the up-flow zone, whereas on the western side of the field there seems to be a cold flow pattern.

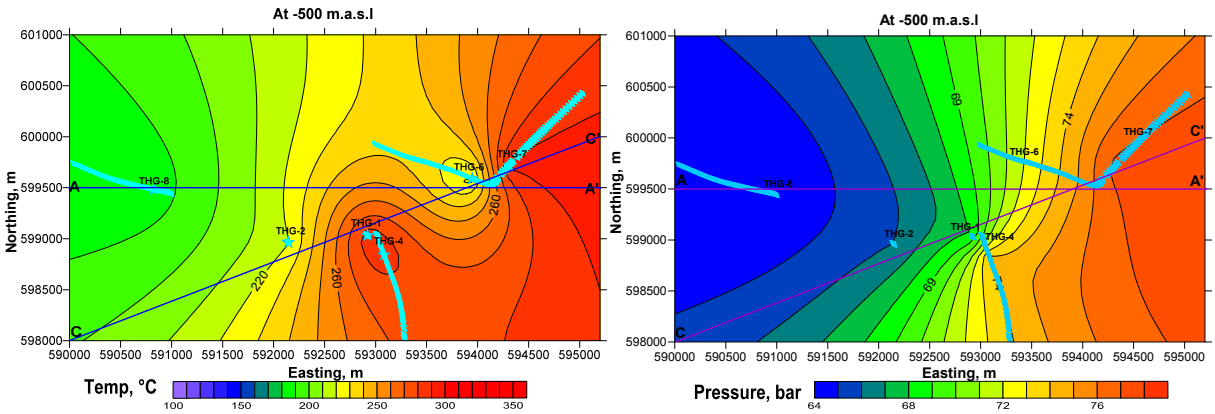

FIGURE 12: Temperature (left) and pressure (right) maps at 500 m b.s.l.

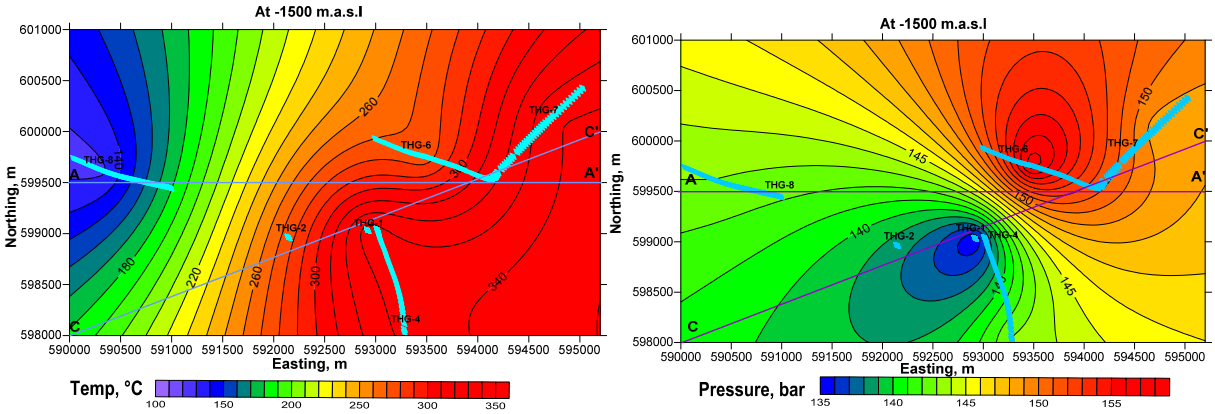

FIGURE 13: Temperature (left) and pressure (right) maps at 1500 m b.s.l.

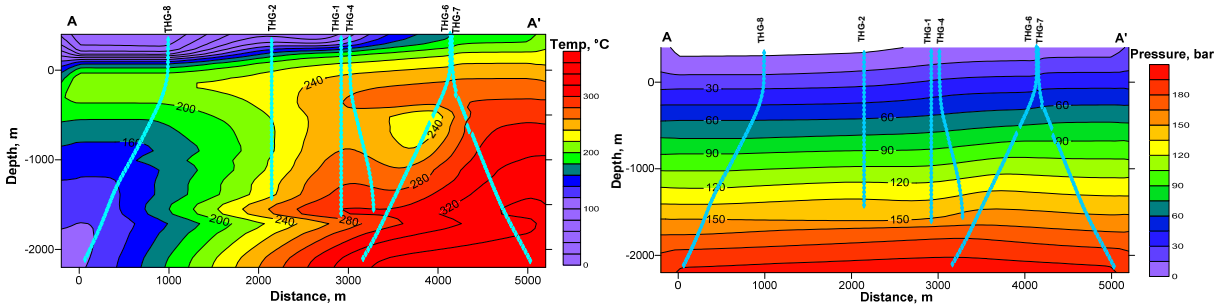

FIGURE 14: Vertical cross-section A-A' for temperature (left) and pressure (right)

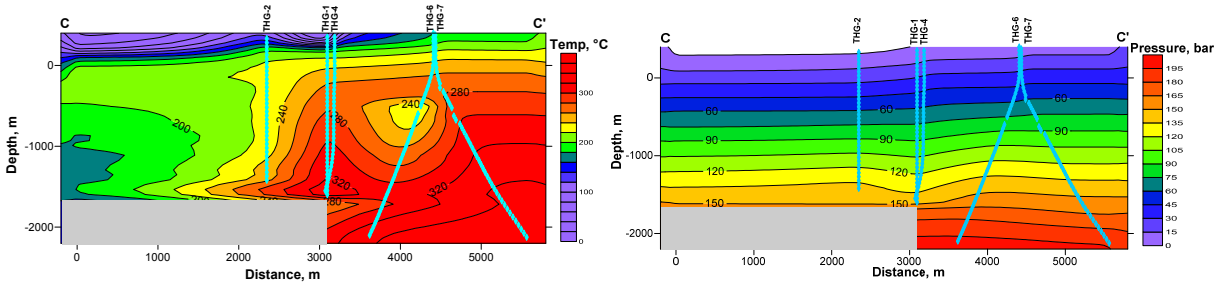

FIGURE 15: Vertical cross-section C-C' for temperature (left) and pressure (right)

It can also be observed from the vertical sections (A-A' and C-C') that at depths below 1500 m b.s.l. the temperature is above 300°C in the eastern section of the field where wells THG-1, THG-4, THG-6 and THG-7 are located. In the top part of the field area, from well THG-1 towards the location of well THG-8 in the western part of the field, there exists a cold pattern, probably due to the cold aquifer at around a depth of 0-500 m.

4. INJECTION WELL TESTING

4.1 Theoretical background

Well testing is performed in order to monitor the pressure response in a reservoir when it is subjected to injection or production. The main purpose is to evaluate the properties that govern the nature of the reservoir, flow characteristics and deliverability of the well. The parameters that are involved are permeability, storativity, transmissivity, wellbore skin, wellbore storage, fracture properties, porosity, initial pressure and reservoir boundaries. The well testing yields more information about the reservoir volume, boundaries, deliverability and recharge when the test lasts for a longer period. To estimate all these parameters, mathematical models need to be developed to simulate the reservoir response. A pressure diffusion equation is the basis for all models. This method is, therefore, often referred to as pressure transient analysis or well test theory.

The pressure diffusion equation is used to calculate the pressure (p) in the reservoir after a given time (t) and at a certain distance (r) from an injection (or production) well receiving (or producing) fluid at a specific rate (Q). The following assumptions are made to simplify the derivation of the equation:

- Horizontal radial flow;
- Darcy's Law applies;
- Homogeneous and isotropic reservoir and isothermal condition;
- Single phase flow and small pressure gradient;
- Constant permeability (k), porosity (φ), fluid viscosity (μ) and total compressibility (c_t); and
- The force of gravity is negligible.

The pressure diffusion equation is derived by combining the equations from the three laws that govern it:

a) Law of conservation of mass (mass in – mass out = mass rate of change):

$$\left(\rho Q + \frac{\partial(\rho Q)}{\partial r}dr\right) - \rho Q = 2\pi r dr \frac{\partial(\rho\varphi h)}{\partial t} \quad or \quad \frac{\partial(\rho Q)}{\partial r} = 2\pi r h \frac{\partial(\varphi\rho)}{\partial t} \tag{1}$$

b) Darcy's law (conservation of momentum):

$$Q = \frac{2\pi r h k}{\mu}\frac{\partial p}{\partial r} \tag{2}$$

c) Fluid compressibility (equation relates the pressure to density at a constant temperature)

$$c_r = \frac{1}{1-\varphi}\frac{\partial\varphi}{\partial p} \quad and \quad c_w = \frac{1}{\rho}\frac{\partial\rho}{\partial p}, \quad then \quad c_t = \varphi c_w + (1-\varphi)c_r \tag{3}$$

This is reduced to:

$$\frac{1}{r}\frac{\partial}{\partial r}\left(r\frac{\partial p}{\partial \rho}\right) = \frac{\mu c_t}{k}\frac{\partial p}{\partial t} = \frac{S}{T}\frac{\partial p}{\partial t} \quad or \quad \frac{\partial^2 p}{\partial r^2} + \frac{1}{r}\frac{\partial p}{\partial r} = \frac{\mu c_t}{k}\frac{\partial p}{\partial t} = \frac{S}{T}\frac{\partial p}{\partial t} \tag{4}$$

$$S = c_t h \quad and \quad T = \frac{kh}{\mu} \tag{5}$$

where ρ = Density (kg/m^3);
Q = Volumetric flow rate (m^3/s);
φ = Porosity (-);
c_t = Total compressibility (Pa^{-1});
c_r = Rock compressibility (Pa^{-1});
c_w = Water compressibility (Pa^{-1});
T = Transmissivity (m^3/(Pa s));
S = Storativity (m/Pa = m^3/(m^{2}Pa) = m^3/N);
μ = Dynamic viscosity (Pa s);
k = Permeability (m^2); and
h = Reservoir thickness (m).

The pressure diffusion equation, given by Equation 4, is the important equation for well test analysis. It is one-dimensional and a second order partial differential equation. Hjartarson (1999) described in detail all mathematical solutions and models involving pressure transient analysis, which is beyond the scope of this project paper. The parameters estimated through the analysis of well tests are described in detail below:

Transmissivity (*T*) is one of the greatest interests in well testing since it determines the ability of the reservoir to deliver fluid. Therefore, if the transmissivity is high, pressure changes diffuse rapidly through the reservoir and vice versa.

Storativity (*S*) is the ability to store a volume of fluid in the reservoir and the amount of fluid that can be released with a change in pressure and area. It has a great impact on how fast the pressure wave can travel within the reservoir.

The injectivity index (*II*) is defined as the change in the injection flow rate divided by the change in stabilized reservoir pressure and has the unit [(L/s)/bar]. It is used to estimate how well a borehole is connected to a surrounding reservoir and is represented mathematically as: $II = \left|\frac{\Delta Q}{\Delta P}\right|$.

Wellbore storage (*C*) refers to the volume of fluid that the wellbore itself will produce due to a given pressure drop. This mostly occurs due to fluid expansion or changing of fluid level in the well. It is represented mathematically as $C = \Delta V / \Delta P$ and has the unit [m^3/Pa].

Skin factor (*s*) is a variable used to quantify the permeability of the volume immediately surrounding a well. It measures how good a connection the well has to the reservoir. A positive value for the skin factor reflects that the well is damaged and a negative value is characteristic for a stimulated well.

Radius of investigation (r_e) is the approximate distance at which the pressure response from the well becomes undetectable. Therefore, this radius defines the area around the well being investigated, although the value of the parameter should be regarded more qualitatively. When boundary effects are seen in the data, the approximate distance to the boundary will define the radius of investigation.

Before the advance of computers, transient analysis was done manually using graphical techniques based on semi-log and log-log plots; only the simplest of these manual techniques are still used. Now the analysis is done through computer software which gives a great variety of options for analysing the system.

4.2 Well Tester software

Well Tester is a program that was written at Iceland GeoSurvey (ÍSOR) to handle data manipulation and analysis of well tests (mainly multi-step injection tests) in Icelandic geothermal fields. The process is divided into five (or in some cases six) simple steps that range from setting initial conditions to modelling and giving a final report (Júlíusson et al., 2008).

The flow models in Well Tester are based on the simplified assumptions made for the pressure diffusion equation. Also, Well Tester is only made to handle well tests where the injection (or production) rate can be assumed to have changed in steps, i.e. Well Tester cannot use flow rate time series from an input file.

The program is easy and user friendly since it has a window based graphical user interface. The process can be easily followed as it was developed in a step-wise fashion, beginning with loading of input data, followed by the setting up of steps and adjusting them. The next step after that is modifying the data set, followed by the actual modelling.

4.3 Injection test analysis

Injection well testing analyses were done only for two wells (THG-7 and THG-8), since they are new wells and these analyses have not yet been performed for them. Injection rates before and after testing, as well as the pressure response at the end of each step tested for THG-7 and THG-8 are summarized in Table 3. Figures 16 and 17 show the pressure response during the injection steps for THG-7 and THG-8, respectively. Different model types were considered and a nonlinear regression analysis was performed to find the parameters that best fit the gathered data. Tables 4 and 5 summarise the model and initial parameters that were selected for the injection well test analysis of these two wells.

Well Tester requires an initial estimate for the parameters, which should preferably be good estimated values so as to get meaningful results from the well test. However, if the estimations are incorrect, it does not affect the results significantly. The initial parameter values used for this analysis are shown in Table 5.

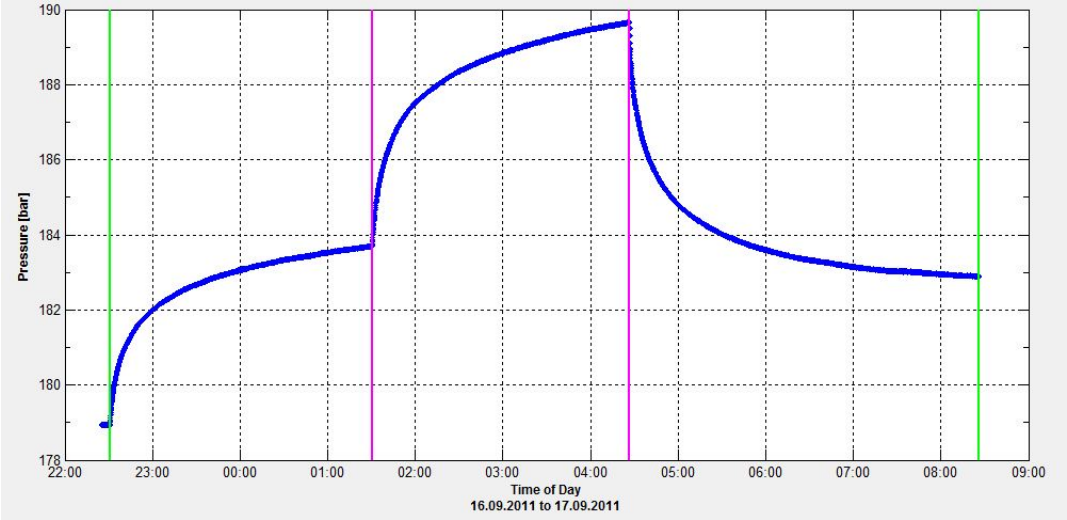

FIGURE 16: Measured pressure at 2492 m depth
in well THG-7 during injection testing

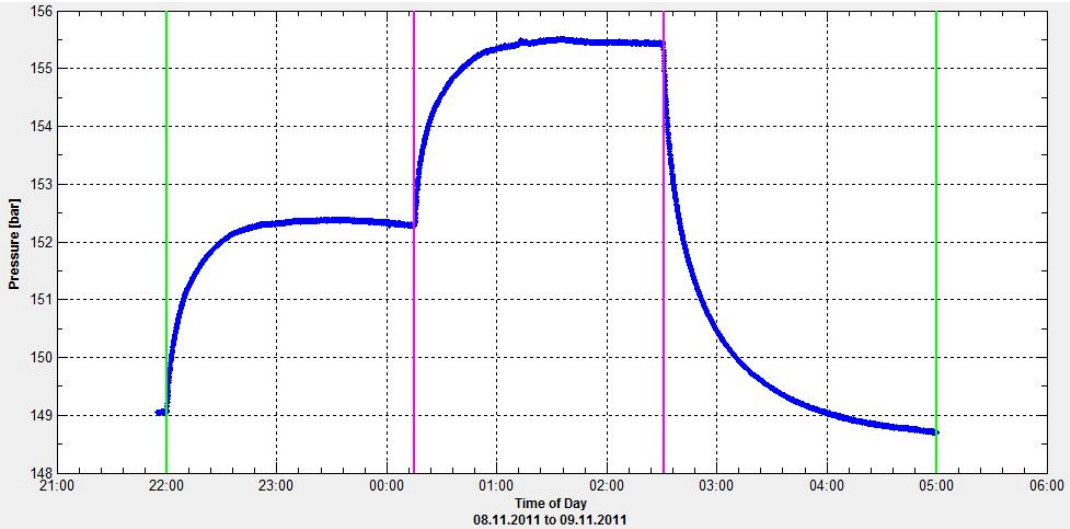

FIGURE 17: Measured pressure at 1780 m depth
in well THG-8 during injection testing

TABLE 3: Summary of pressure response measured during each step for wells THG-7 and THG-8

	Time period	Duration (hr)	Injection (l/s)	Pressure at the end of step (bar-g)	Injectivity index ((l/s)/bar)
THG-7, Tested 16-17 September 2011					
Initial injection		-	20.2	178.96	-
Step 1	16.09 22:30 - 17.09 01:30	2.99	20.2	183.8	2.10
Step 2	17.09 (01:30 - 04:27)	2.94	30.3	189.7	1.65
Step 3	17.09 (04:27 - 08:26)	3.98	40.0	182.9	2.27
THG-8, Tested 08- 09 November 2011					
Initial injection		-	20.0	149.06	-
Step 1	08.11 22:00 - 09.11 00:15	2.26	20.0	152.3	2.16
Step 2	09.11 (00:15 - 02:31)	2.26	27.0	155.5	2.49
Step 3	09.11 (09:11 - 05:00)	2.48	35.0	148.7	1.67

For both wells (THG-7 and THG-8), the results of the modelling are presented for each step. Figures 18 to 21 show the pressure measured for each step on a linear scale using a logarithmic timescale, the pressure change on a logarithmic scale using a logarithmic timescale, together with the derivative of the pressure response multiplied by the time passed. The values shown for each parameter are the best estimates from the nonlinear regression analysis of the measured data.

TABLE 4: Summary of model selected for the injection well test analysis

Reservoir	Homogeneous
Boundary	Constant pressure
Well	Constant skin
Wellbore	Wellbore storage

THG-7: The pressure measurements were done at 2492 m measured depth. Figures 18 and 19 are the plots that show the best fit in the model for steps 1 and 3. The parameters estimated from these steps are summarized in Table 6.

TABLE 5: Summary of initial parameters given in Well Tester

Parameter	THG-7	THG-8
Estimated reservoir temperature, T_{est} (°C)	280	280
Estimated reservoir pressure, P_{est} (bar)	184	152
Wellbore radius, r_w (m)	0.16	0.16
Porosity, φ (%)	0.1	0.1
Dynamic viscosity of reservoir fluid, μ (Pa s)	9.72×10^{-5}	9.63×10^{-5}
Compressibility of reservoir fluid, c_w (Pa^{-1})	1.78×10^{-9}	1.88×10^{-9}
Compressibility of rock matrix, c_r (Pa^{-1})	2.44×10^{-11}	2.44×10^{-11}
Total compressibility, c_t (Pa^{-1})	2.0×10^{-10}	2.10×10^{-10}

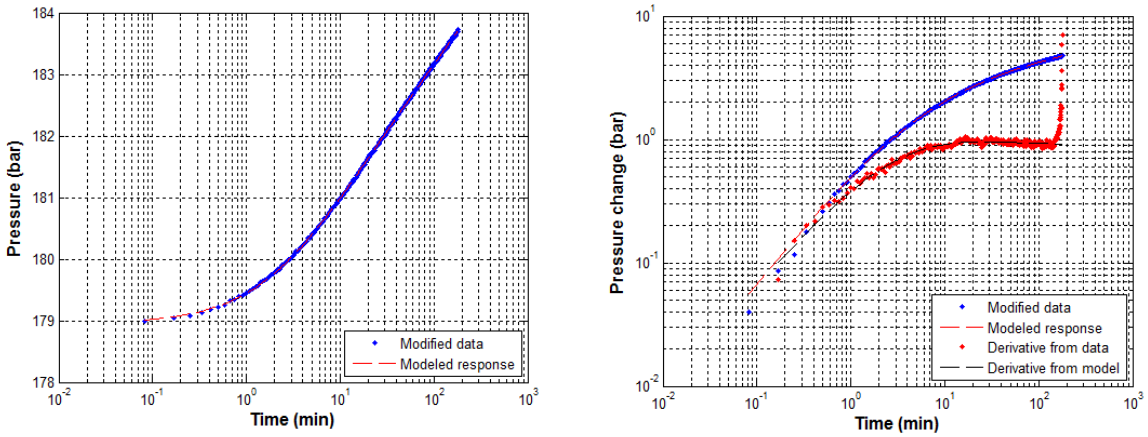

FIGURE 18: Well THG-7, fit between model and collected data for step 1 using a logarithmic time scale (left) and log-log scale (right)

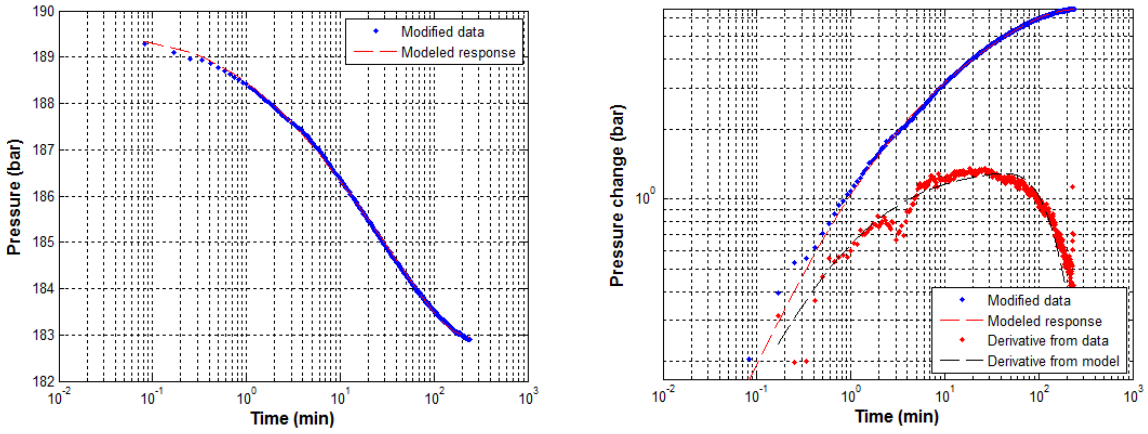

FIGURE 19: Well THG-7, fit between model and collected data for step 3 using a logarithmic time scale (left) and log-log scale (right)

TABLE 6: Summary of reservoir parameters estimated using nonlinear regression model for well THG-7

Parameter	Step 1	Step 2	Step 3	Best estimate
Transmissivity, T (m^3/(Pa.s))	9.02×10^{-9}	6.96×10^{-9}	8.72×10^{-9}	8.2×10^{-9}
Storativity, S ($m^3/(m^2Pa)$)	7.12×10^{-8}	8.03×10^{-8}	3.96×10^{-8}	7.0×10^{-8}
Radius of investigation, r_e (m)	114	114	67	100
Skin factor, s	-3.17	-2.97	-3.62	-3.25
Wellbore storage, C (m^3/Pa)	7.79×10^{-6}	7.74×10^{-6}	3.18×10^{-6}	7.0×10^{-6}
Injectivity index, II ((L/s)/bar)	2.13	1.65	2.29	2.02
Reservoir thickness, h (m)	356	402	198	350
Permeability, k (m^2)	2.46×10^{-15}	1.69×10^{-15}	4.28×10^{-15}	2.5×10^{-15}
Porosity, φ	0.1	0.1	0.1	0.1

THG-8: The pressure measurements were done at 1780 m measured depth. Figures 20 and 21 are the plots that show the best fit in the model for steps 2 and 3. The parameters estimated from these steps are summarized in Table 7.

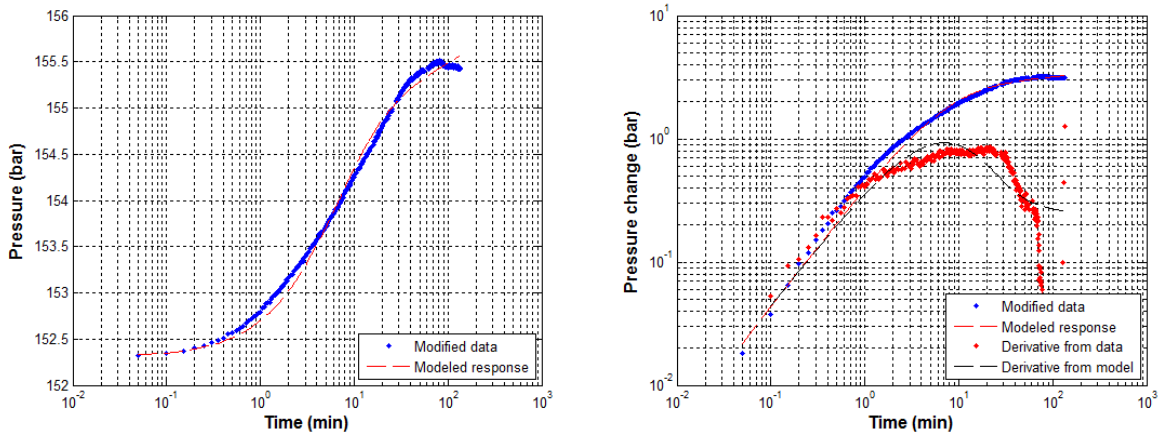

FIGURE 20: Well THG-8, fit between model and collected data for step 2 using a logarithmic time scale (left) and log-log scale (right)

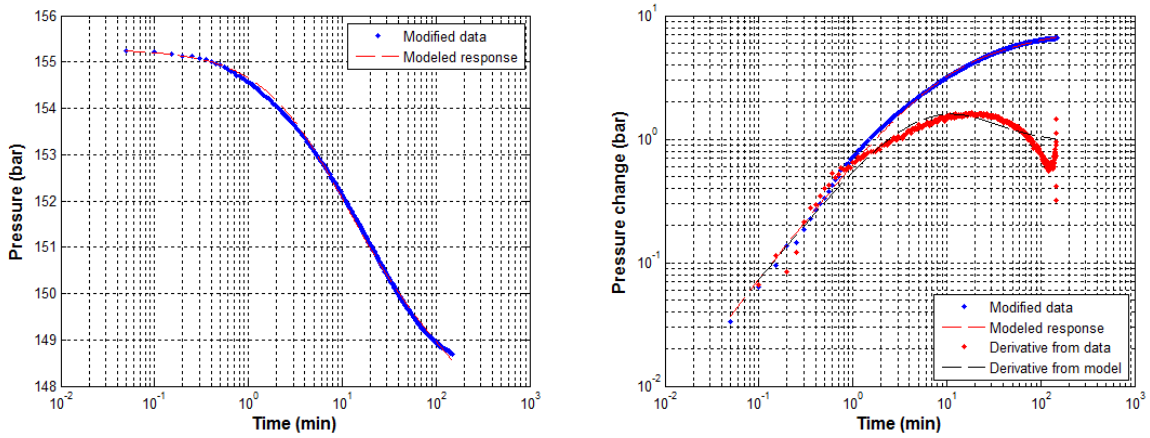

FIGURE 21: Well THG-8, fit between model and collected data for step 3 using a logarithmic time scale (left) and log-log scale (right)

TABLE 7: Summary of reservoir parameters estimated using nonlinear regression model for well THG-8

Parameter	Step 1	Step 2	Step 3	Best estimate
Transmissivity, T (m^3/(Pa.s))	5.81×10^{-9}	7.23×10^{-9}	6.59×10^{-9}	6.5×10^{-9}
Storativity, S ($m^3/(m^2Pa)$)	1.27×10^{-8}	1.42×10^{-8}	1.61×10^{-8}	1.4×10^{-8}
Radius of investigation, r_e (m)	15	17	22	18
Skin factor, s	-2.83	-2.84	-2.45	-2.7
Wellbore storage, C (m^3/Pa)	4.88×10^{-6}	5.09×10^{-6}	6.44×10^{-6}	5.5×10^{-6}
Injectivity index, II ((L/s)/bar)	2.12	2.53	1.68	2.1
Reservoir thickness, h (m)	604	674	765	680
Permeability, k (m^2)	9.27×10^{-16}	1.03×10^{-15}	8.29×10^{-16}	1.0×10^{-15}
Porosity, φ	0.1	0.1	0.1	0.1

5. PRODUCTION TEST

5.1 Theoretical background

Production well tests are conducted to determine the production capacity and to analyse the flow characteristics of a well. The tests are done after a geothermal well has been drilled and allowed to warm up for some time. Then a discharge test is conducted by starting the well's flow, followed by measurements to calculate the fluid flow at different wellhead pressures. The first step in flow testing is starting the well discharge by opening up the well. This allows flow to the atmosphere for a short time and helps to clear debris from the well. It can also help to determine the most suitable equipment for long-term testing. Then the well is discharged into a silencer which is designed to reduce the noise level resulting from the discharge. In addition, the silencer acts as a water-steam separator at atmospheric pressure. The lip pressure is measured at the end of the discharge pipeline as it enters the silencer and measurement of water separated from the silencer is done in a V-notch weir while the steam is allowed to escape into the atmosphere.

Russell James's formula is an empirical formula developed in 1960 which relates mass flow, enthalpy, discharge pipe area and lip pressure as follows (Grant and Bixley, 2011):

$$\frac{GxH_t^{1.102}}{P_{lip}^{0.96}} = 184, \;\; G = W/A \tag{6}$$

where G = Mass flow per unit area (kg/scm^2);
W = Mass flow (kg/s);
H = The enthalpy (kJ/kg);
A = The cross-section area of the pipe (cm^2); and
P_{lip} = Lip pressure, bar-absolute.

The separated water flow W_w is the water separated at atmospheric pressure from the total well flow with enthalpy H_t. Therefore,

$$W = W_w \frac{H_s - H_w}{H_s - H_t} \tag{7}$$

where H_s = Enthalpy of steam (kJ/kg); and
H_w = Enthalpy of water

Combining Equations 6 and 7 gives:

$$\frac{W_w}{AP_{lip}^{0.96}} = \frac{184}{H_t^{1.102}} \frac{H_s - H_t}{H_s - H_w} \tag{8}$$

The enthalpies H_s and H_w can be found in steam-tables for corresponding pressure (or temperature) and the only unknown is H_t from which the electric power can be calculated. The total mass flow, W, is calculated by relating the water mass flow, W_w as in Equation 9:

$$W = \frac{W_w}{1 - X} \frac{H_s - H_t}{H_s - H_w} \quad and \quad X = \frac{H_t - H_w}{H_s - H_w} \tag{9}$$

where X = The steam mass fraction.

5.2 Production test analysis for THG-6

In well THG-6, initial self-sustaining discharge was possible due to the presence of wellhead pressure. The well was tested with two lip pressure pipes, 15 and 10 cm, which attained wellhead pressure stability for each pipe. The lip pressure pipe with a diameter of 15 cm was used in a test that started in November 2008 and lasted for about eight months. Then the well was closed until October 2010 and the 10 cm lip pressure diameter was used for a test which lasted for more than six months (Figure 22). Table 8 shows average outputs for wellhead pressure, water flow, steam flow, total flow rate and total enthalpy of each diameter of lip pressure pipe used during the tests.

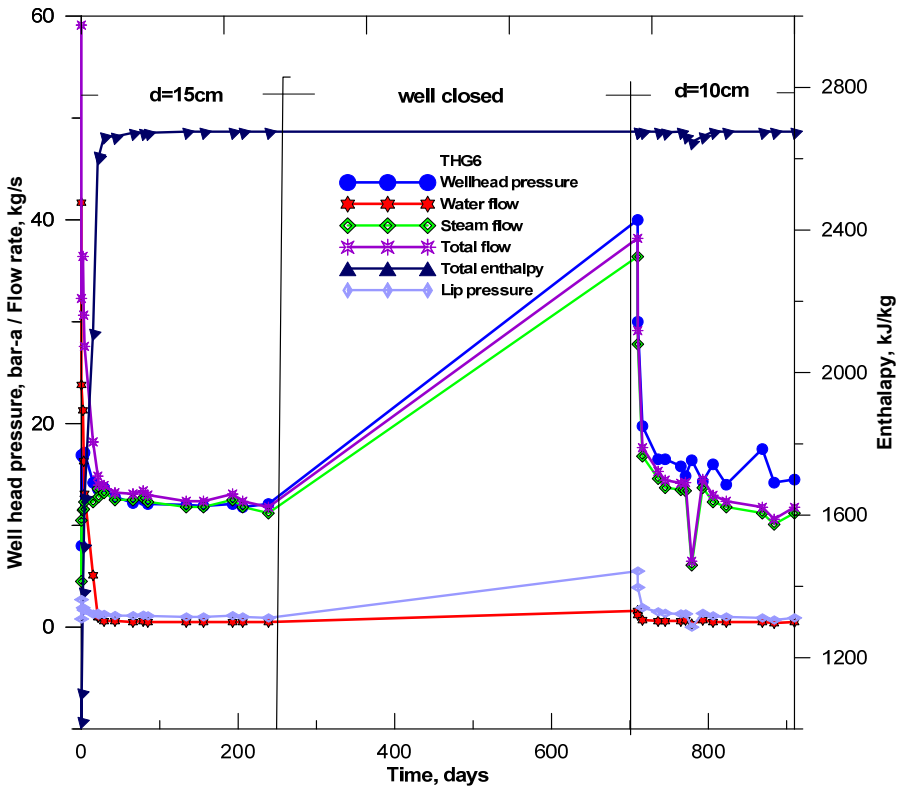

FIGURE 22: Well THG-6 production tests history

TABLE 8: Summary of average outputs for well THG-6

Lip pipe diameter (cm)	Wellhead pressure (bar-a)	Water flow (kg/s)	Steam flow (kg/s)	Total mass flow (kg/s)	Total enthalpy (kJ/kg)
15	12.1	~0.5	12.1	12.4	2676
10	14.2	~0.5	11.2	11.8	2676

6. GEOTHERMAL RESOURCE ASSESSMENT

The Volumetric method was applied in this project paper to update the geothermal resource assessment of the Theistareykir high-temperature field which was previously assessed in 2008 by Gudmundsson et al. The main results from the 2008 assessment were that most likely the production capacity of Theistareykir geothermal system is 350 MWe for 30 years, 210 MWe for 50 years and 100 MWe for 100 years production period. It was also predicted that the system could produce at least 240 MWe (90% limit) when 30 years is considered as a production period; if 50 and 100 year periods are considered, the system could produce at least 150 and 70 MWe, respectively. The results covered a very wide range, mainly due to uncertainty in the surface area of the region and the recovery factor. The uncertainty was expected to decrease with further drilling. The drilling of two wells (THG-7 and THG-8) in 2011 has helped to decrease this uncertainty to some extent; however, more drill work is needed in the western part of the field to understand the extension of the colder zone below 800 m that was encountered in well THG-8.

6.1 Theory of volumetric method

A geothermal resource is considered the portion of accessible thermal energy that could be extracted from a depth shallow enough by employing the available technology for man's use economically (Muffler and Cataldi, 1978). Muffler and Cataldi (1978) identified four methods for assessing geothermal resources: volume method, surface heat flux, planar fracture and magmatic heat budget. The volume method is well established and commonly used for initial stage assessment when data are limited. However, it is still the main assessment method in some countries (Gylfadóttir and Halldórsdóttir, 2012).

The method involves the calculation of the thermal energy in a given volume of rock and fluid and the estimation of total heat stored in the reservoir's volume. The total heat in the geothermal system is calculated by integrating the product of the heat capacity and temperature with respect to the volume of the geothermal system (Halldórsdóttir et al., 2010).

$$Q = \oint_v C[T - T_0]\, dV \tag{10}$$

where Q = The heat contained in the geothermal system (J);
C = The heat capacity per unit volume (J/m^3°C);
T = The reservoir temperature (°C); and
T_0 = The reference (cut-off) temperature (°C).

T_0 could be the mean annual temperature or surface temperature or the flash temperature in a geothermal power plant.

Assuming that the heat capacity and temperature are homogeneous in the horizontal directions and vary only vertically, then the heat content, Q, can be calculated by integrating the heat capacity per unit volume $C_{(z)}$, multiplied by the difference of the estimated temperature curve $T_{(z)}$ in the system and the reference temperature T_0.

$$Q = A \int_{z_0}^{z_1} C(z)[T(z) - T_0]\, dz \tag{11}$$

where A = The surface area of the geothermal system (m^2).

For simplicity, the system is often divided into different layers where the heat capacity is constant in each layer and depends only on the specific heat and density of the rock and water, respectively.

$$C = \rho_w s_w \varphi + \rho_r s_r (1 - \varphi) \quad (12)$$

where φ = The porosity of the rock,
ρ_w, ρ_r = Density of water and rock, respectively (kg/m^3); and
s_w, s_r = Specific heat of water and rock, respectively (J/kg°C).

According to James (1970), it is convenient to assume that the temperature curve in many high-temperature geothermal fields follows a curve shaped like a boiling point curve. Equation 13 describes a temperature profile shaped like the boiling point curve. X in the equation describes the ratio factor of how much the temperature deviates from the true boiling point curve, and runs from zero to one, $zdelta$ is a translation in the z direction in order to meet the upper boundary conditions, $T(z_0)$ at z_0.

$$T(z) = X \cdot 69.56\ (z - zdelta)^{0.2085} \quad (13)$$

The recovery factor, R, indicates the portion of the total heat in the system that can be recovered.

$$Q_R = RAC \int_{z_0}^{z_1} [T(z) - T_0] dz \quad (14)$$

From the recoverable heat of the geothermal system, only a small portion can be used for electric generation. Therefore, an electric utilization constant η_e which gives us the electric energy can be defined as:

$$Q_e = \eta_e Q_R \quad (15)$$

This gives the electric power.

$$P = \frac{Q_e}{t} \quad (16)$$

Where t = The production time of the electric power (s).

6.2 Monte Carlo calculations

The Monte Carlo method was named after the Monte Carlo casino and introduced in the 1940s by a scientist working on the nuclear weapon project at the Los Alamos National Laboratory (Gylfadóttir and Halldórsdóttir, 2012). The method involves random sampling of each variable out of their probability distribution to produce one possible outcome. If the process is repeated several times a discrete probability distribution for the outcome begins to form. The variables used in the volumetric method are usually uncertain; it is, therefore, convenient to define the range of possible values for each variable.

6.3 Estimation of Monte Carlo variables for Theistareykir field

In order to perform the Monte Carlo calculations for volumetric assessment we have to estimate the values for the following variables:

- Surface area of the geothermal system;
- Thickness of the geothermal system;
- Porosity of the rock in the system;
- Mean physical characteristics of the rock and water in the system, which are the specific heat and density of rock and water;
- Heat distribution throughout the reservoir;
- Recovery factor and reference temperature; and
- Electric utilization coefficient and production time.

From the surface resistivity survey in the area and surface geology, the surface area for the Theistareykir geothermal field can be estimated. The low-resistivity cap in the area has been observed and, at a depth of 800-1000 m, it has an area of approximately 45 km^2 (Figure 4). Surface geology showed that the geothermal activity covers an area of about 20 km^2 (Figure 2). The northwest part of the geothermal field, where well THG-8 was drilled, was excluded because well THG-8 turned out to be cold, with a temperature below 170°C at depths greater than 800 m. This decreases the surface area to about 40 km^2 which is taken as the maximum value. The active geothermal area at the surface is about 10 km^2 (Figure 2) and is considered a minimum surface area.

The eight deep wells drilled in the Theistareykir area have depths in the range of 1700-2800 m. It is assumed that most geothermal systems have a thickness of 3000 m as this is the depth that can easily be reached by modern technology. Therefore, the maximum reservoir thickness is estimated as 3000 m while the minimum is taken as 2500 m, due to the cold inflow zone encountered at a depth above 500 m.

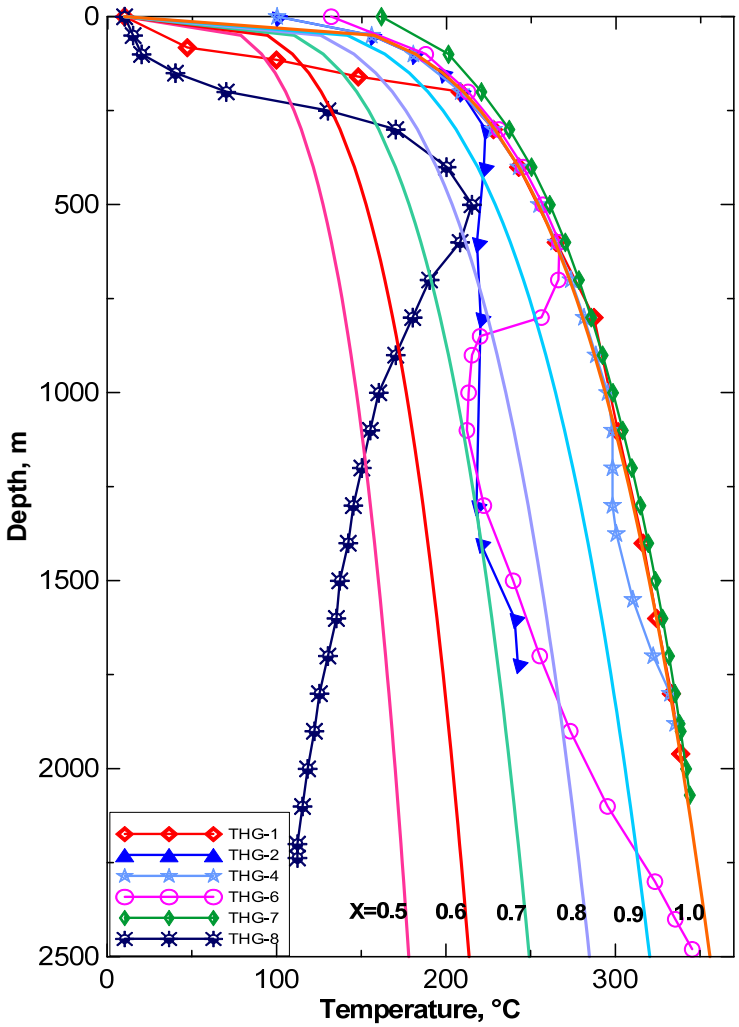

FIGURE 23: Formation temperatures of six wells in Theistareykir field and *T(z)* for different values of *X*

The bedrock in the area was divided into basaltic hyaloclastite from subglacial eruptions during the Ice Age, interglacial lava flows and recent lava flows (Ármannsson et al., 1986). Halldórsdóttir et al. (2010) suggested that the porosity of the basaltic lava is in the range 5-15%, and that of hyaloclastite is from 15 to 35% in fresh tuff; below 900-1200 m depth, intrusions of very low porosity are more common in Iceland. Therefore, for this Monte Carlo calculation the porosity of the rock is considered to be in the range of 5-20%, with the mostly likely value of 10% which is also in agreement with the porosity found by Well Tester for the injection tests of THG-7 and THG-8.

Figure 23 shows the formation temperatures of six wells in the Theistareykir field and *T(z),* according to Equation 13 for different values of *X; T(z$_0$)* is given as 10°C. The formation temperatures fall in the range, where X = 0.7-1.0. The common process in Iceland is to flash the geothermal fluid at 10 bars, which corresponds to a temperature of roughly 170°C. Therefore, the cut-off temperature was set to this value. According to Muffler (1977 and 1979) the recovery factor is controlled by the porosity and permeability and has a linear relationship with the porosity, usually given values between 10 and 25%. Therefore, a rock with mean porosity of 10% should have a recovery factor of 25%. The electric utilization coefficient can be estimated from the cut-off temperature (170°C) and is chosen to be 12% in this calculation. Table 9 shows the variables applied in the volumetric calculations.

TABLE 9: Parameters used in the Monte Carlo calculations

Variable	Distribution type	Minimum	Mostly likely	Maximum
Surface area (km^2)	Triangular	10	20	40
Thickness (m)	Constant distr.	2500	-	3000
Porosity (%)	Triangular	5	10	20
Cut-off temperature (°C)	Fixed	-	170	-
Recovery factor (%)	Triangular	10	20	25
Utilization coefficient (%)	Fixed	-	12	-
Specific heat of rock (J/(kg°C))	Fixed	-	900	-
Specific heat of water (J/(kg°C))	Fixed	-	6648	-
Density of rock (kg/m^3)	Fixed	-	2800	-
Density of water (kg/m^3)	Fixed		662	
Boiling curve ratio (%)	Triangular	70	85	100
Production time (years)	Fixed	-	30, 50	-

6.4 Results of the volumetric calculations

Two production periods (30 and 50 years) were used for the volumetric calculations. A total of 100,000 random outcomes were considered for each calculation and the results are presented as a discrete probability distribution and a cumulative probability distribution in Figures 24 and 25, respectively. According to Figure 24, it is most likely that the electric power production is 230 MWe for 30 years and 135 MWe for 50 years with approximately 13 and 14% probability, respectively. The statistics show that the 90% confident range is 100-500 and 60-290 MWe for 30 and 50 years, respectively.

Figure 25 shows the cumulative probability distribution and the statistics predict with 90% probability that at least 160 MWe (90% limit) can be produced for a 30 year production period and at least 90 MWe for 50 years. Table 10 summarises the statistical results for the probability distribution for electric power production for 30 and 50 years at the Theistareykir high-temperature field.

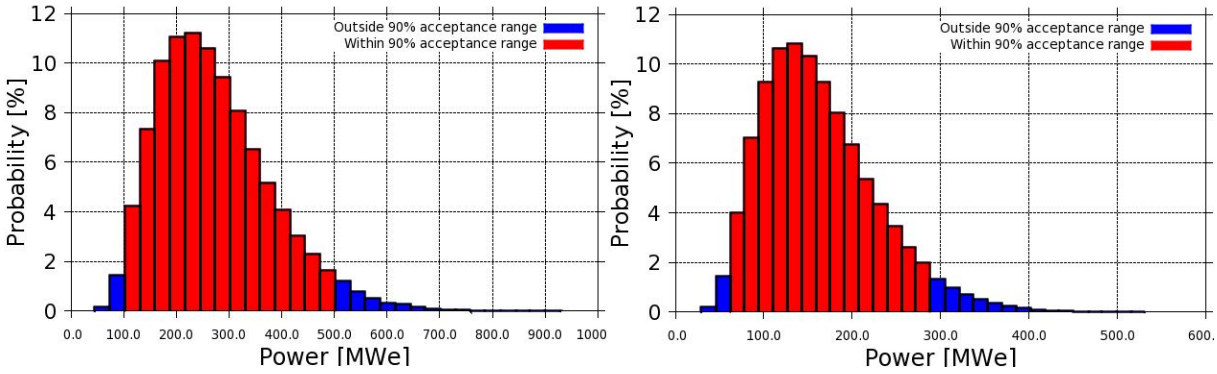

FIGURE 24: Probability distribution for electric power production for 30 (left) and 50 (right) years

TABLE 10: Statistical parameters for the probability distribution for electric power production for the Theistareykir high-temperature field estimated by the Monte Carlo calculation

Statistical sizes	Values (MWe) 30 years	Values (MWe) 50 years
Mostly likely value	230	135
90% confident range	100 - 500	60 - 290
Mean value	273	164
Median value	257	154
Standard deviation	109	65
90% limit	160	90

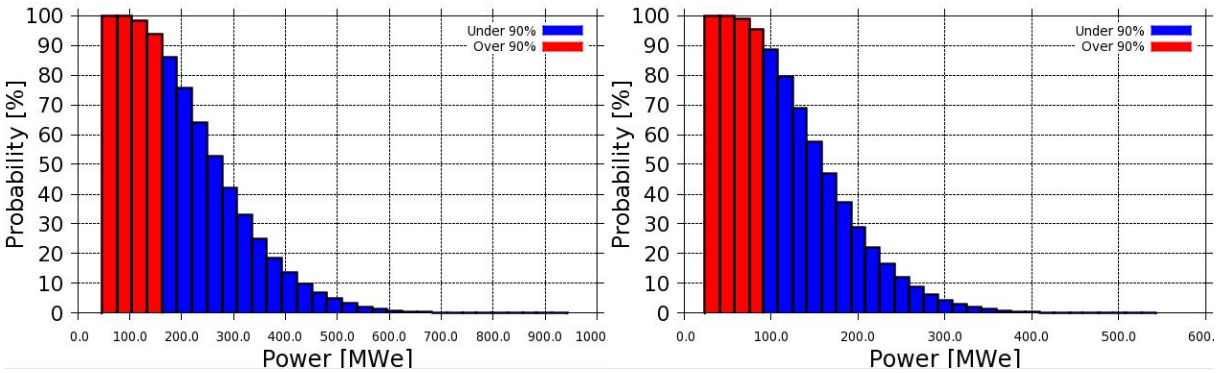

FIGURE 25: Cumulative probability distribution for electric power production for 30 (left) and 50 (right) years

7. DISCUSSION AND CONCLUSIONS

Based on both the temperature and pressure analyses done in six wells, it was revealed that the temperature is increasing in a northeast direction and decreases in a northwest direction. The up-flow zone is located near well THG-1 and spreads in a northeast direction while it is very limited in the northwest direction. Temperature below 1500 m b.s.l. is above 300°C on the eastern side (where wells THG-1, THG-4, THG-6 and THG-7 are located) of the reservoir spreading in a northeast direction. In the northwest part where THG-8 is situated, the temperature is below 170°C down to 800 m b.s.l. depth. Generally, the area consists of a cold inflow at a shallow depth.

Injection well test analyses done for wells THG-7 and THG-8 gave the best results for a model with a constant boundary pressure. The transmissivity values obtained in the injection well tests for these wells are in order of 10^{-8} $m^3/(Pa\ s)$ which are common values for wells drilled in Icelandic geothermal reservoirs, as suggested by Júlíusson et al. (2008). Their skin factor values are negative, which indicates that the wells are in good connection with the reservoir, a result that may be due to stimulation of the wells. Generally, the two wells analysed are also characterised by good permeability as well as storativity.

Resource assessment performed for the Theistareykir geothermal field using the volumetric method and Monte Carlo calculations estimated that approximately 230 MWe could be generated for the 30 year production time with 90% confident range of 100-500 MWe. If the production time is extended to 50 years it was estimated that about 135 MWe could be produced with a 90% confident range of 60-290 MWe. The statistics estimated in the 2008 study by Gudmundsson et al., estimated that most likely electric production could be 350 MWe for 30 years and 210 MWe for 50 years production period. The difference in the estimated values can be explained by the decrease of the reservoir volume. The reservoir thickness in the 2008 study was 3000 m while in this study it is between 2500 and 3000 m. Recent drilling has reduced the reservoir surface area, lowering the estimated power production for the system as well as the uncertainty of the outcome. However, more drill work is still required in the western part of the field to confirm the extension of the colder zone encountered in well THG-8.

ACKNOWLEDGEMENTS

I would like to express my sincere gratitude to the UNU-GTP Director, Dr. Ingvar B. Fridleifsson, and his deputy, Mr. Lúdvík S. Georgsson, for giving me the opportunity to participate in this specialized training programme. I am grateful to the UNU-GTP staff, Ms. Thórhildur Ísberg, Mr. Ingimar G. Haraldsson, Mr. Markús A.G. Wilde and Ms. Málfrídur Ómarsdóttir for their incredible support during the whole training and stay in Iceland. Great thanks to my supervisors, Ms. Saeunn Halldórsdóttir and Ms. Sigrídur Sif Gylfadóttir, for their tireless supervision, instructions and guidelines throughout my project. Special thanks to all lecturers, staff members of ÍSOR and Orkustofnun for their comprehensive presentations, and for sharing their knowledge and experiences. And, to my fellow students, we had great moments that will be treasured forever. Many thanks go to the Government of Tanzania and my employer TANESCO for approving my attendance at this training.

Many thanks to my family: my mother, wife, brothers and sister for their endless patience, strong encouragement and continuous support for the whole period of my study and stay in Iceland; you all mean a life to me.

I am grateful to the almighty ALLAH for his protection and guidance during the entire time of my study and stay in Iceland.

Finally, I want to dedicate the work to *Idrissa* - my son.

REFERENCES

Arason, Th., Björnsson, G., Axelsson, G., Bjarnason, J.Ö., and Helgason, P., 2004: *The geothermal reservoir engineering software package Icebox, user´s manual*. Orkustofnun, Reykjavík, 53 pp.

Arnaldsson, A., Halldórsdóttir, S., Kjaran, S.P., and Axelsson, G., 2011: *Calculation of the geothermal system in Theistareykir and preliminary performance.* Iceland GeoSurvey and Vatnaskil Engineering, Reykjavík, report ÍSOR-2011/049 and Vatnaskil 11-08 (in Icelandic*)*, 58 pp.

Ármannsson, H., 2011: The Theistareykir geothermal system, North East Iceland. Case history. *Presented at "Short Course VI on Exploration for Geothermal Resources", organized by UNU-GTP, GDC and KenGen, Lake Naivasha, Kenya,* 11 pp.

Ármannsson, H., Gíslason, G., and Torfason, H., 1986: Surface exploration of the Theistareykir high-temperature geothermal area, with special reference to the application of geochemical methods. *Applied Geochemistry, 1,* 47-64.

Ármannsson, H., Kristmannsdóttir, H., Torfason, H., and Ólafsson, M., 2000: Natural changes in unexploited high-temperature geothermal areas in Iceland. *Proceedings of the World Geothermal Congress 2000, Kyushu-Tohuku, Japan*, 521-526.

Darling, W.G., and Ármannsson, H., 1989: Stable isotope aspects of fluid flow in the Krafla, Námafjall and Theistareykir geothermal systems of northeast Iceland. *Chem. Geol., 76,* 197-213.

Gíslason, G., Johnsen, G.V., Ármannsson, H., Torfason, H., and Árnason, K., 1984: *Theistareykir. Surface exploration of the high-temperature geothermal area.* Orkustofnun, Reykjavík, report OS-84089/JHD-16 (in Icelandic), 134 pp + 3 maps.

Grant, M.A., and Bixley, P.F., 2011: *Geothermal reservoir engineering* (2nd ed.). Academic Press, NY, 349 pp.

Grönvold, K., and Karlsdóttir, R., 1975: *Theistareykir. An interim report on the surface exploration of the geothermal area.* Orkustofnun, Reykjavík, report JHD-7501 (in Icelandic), 37 pp.

Gudmundsson, Á., Gautason, B., Lacasse, C., Axelsson, G., Thorgilsson, G., Ármannsson, H., Tulinius, H., Saemundsson, K., Karlsdóttir, R., Kjaran, S.P., Pálmarsson, S.Ó.,Halldórsdóttir, S., and Egilsson, Th., 2008: *Conceptual model of the Theistareykir geothermal area and evaluation of geothermal resources by volumetric method* (in Icelandic). ÍSOR - Iceland GeoSurvey, Mannvit, and Vatnaskil, report ÍSOR-2008/024, MV-049 and Vatnaskil 08.05, 67 pp.

Gylfadóttir, S.S., and Halldórsdóttir, S., 2012: *Volumetric assessment of geothermal systems.* UNU-GTP, Iceland, unpublished lecture notes.

Halldórsdóttir, S., Björnsson, H., Axelsson, G., Gudmundsson, A., and Mortensen, A.K., 2010: Temperature model and volumetric assessment of the Krafla geothermal field in N-Iceland. *Proceedings of the World Geothermal Congress 2010, Bali, Indonesia,* 10 pp.

Hjartarson, A., 1999: *Analysis of reservoir data collected during reinjection into the Laugaland geothermal system in Eyjafjördur, N-Iceland.* University of Iceland and Orkustofnun, MSc. thesis, Reykjavík, 107 pp.

James, R., 1970: Factors controlling borehole performance. *Geothermics, Sp. Issue, 2-2,* 1502-1515.

Júlíusson, E., Grétarsson, G.J., and Jónsson, P., 2008: *Well Tester 1.0b, user's guide*. ÍSOR – Iceland GeoSurvey, Reykjavík, report ÍSOR-2008/063, 27 pp.

Karlsdóttir, R., Eysteinsson, H., Magnússon, I.Th., Árnason, K, and Kaldal, I., 2006: *TEM soundings at Theistareykir and Gjástykki 2004-2006*. ÍSOR - Iceland GeoSurvey, report ÍSOR-2006/028, 88 pp.

Karlsdóttir, R., and Vilhjálmsson, A.M., 2011: *MT and TEM survey at Theistareykir in 2009*. ÍSOR - Iceland GeoSurvey, report ÍSOR-2011/021, 78 pp.

KMS Technologies, 2008: *Mapping geothermal reservoir using 2-D MT survey in Theistareykir, Iceland.* KMS Technologies, prepared in cooperation with Mannvit.

Layugan, D.B., 1981: *Geoelectrical soundings and its application in the Theistareykir high temperature area.* UNU-GTP, Iceland, report 5, 101 pp.

Muffler, L.P.J., 1977: 1978 USGS geothermal resource assessment. *Proceedings of the Stanford Geothermal Workshop, Stanford University, Stanford, CA*, 3-8.

Muffler, L.P.J. (editor), 1979: Assessment of geothermal resources of the United States - 1978. *US Geological Survey Circular 790*. USGS, Arlington, VA, 163 pp.

Muffler, P., and Cataldi, R., 1978: Methods for regional assessment of geothermal resources. *Geothermics, 7*, 53-89.

APPENDIX I: Estimation of formation temperature and initial pressure for wells ThG-1, THG-2 and THG-4

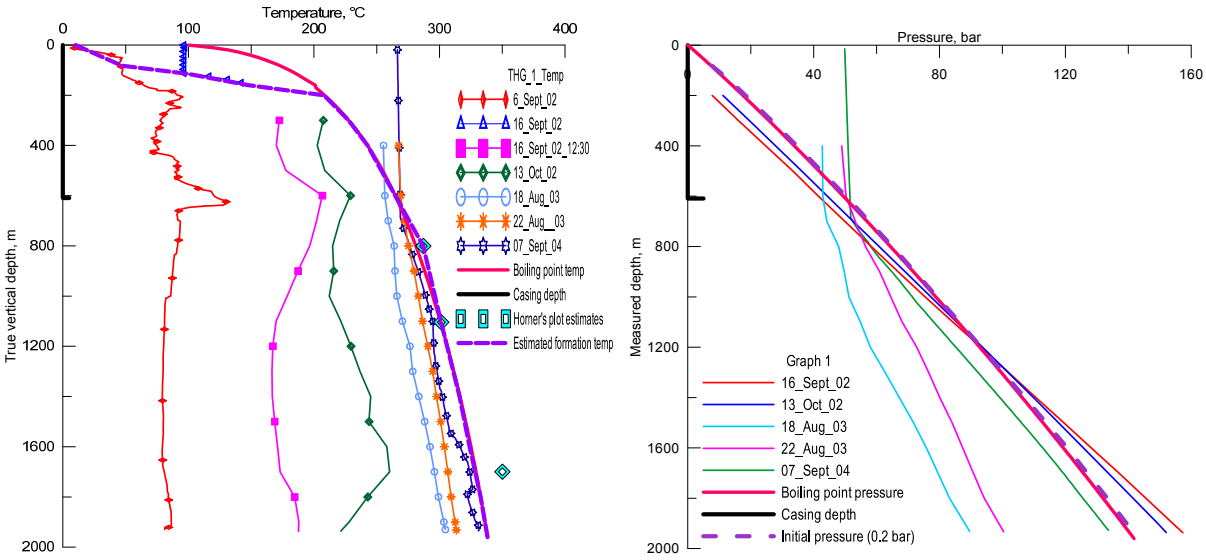

FIGURE 1: Well THG-1, estimated formation temperature (left) and initial pressure (right)

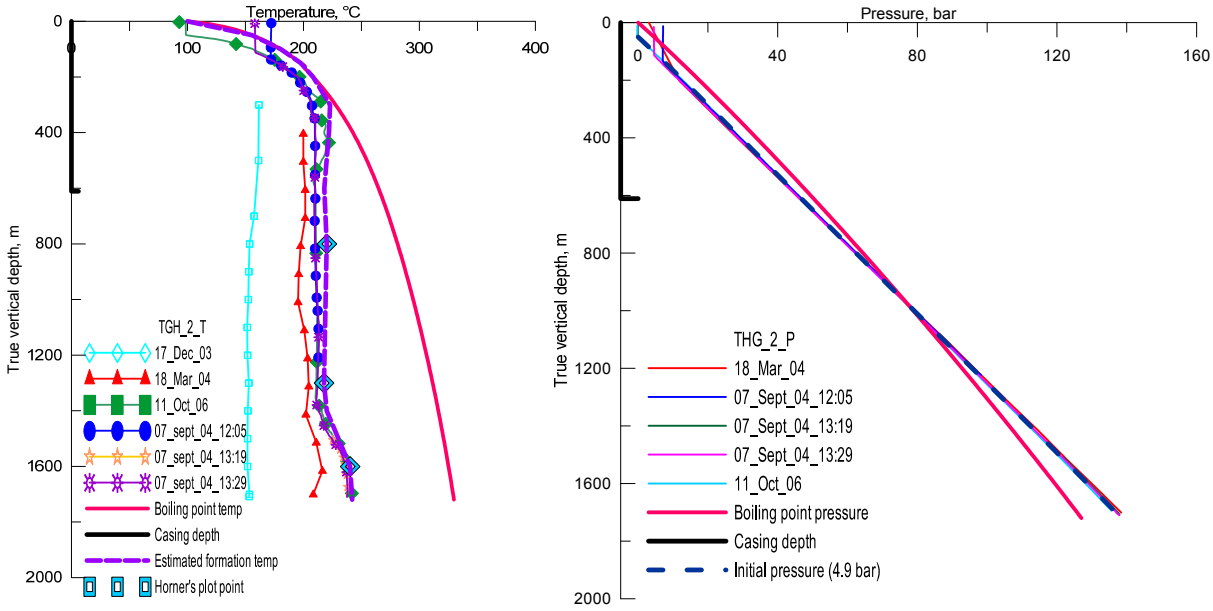

FIGURE 2: Well THG-2, estimated formation temperature (left) and initial pressure (right)

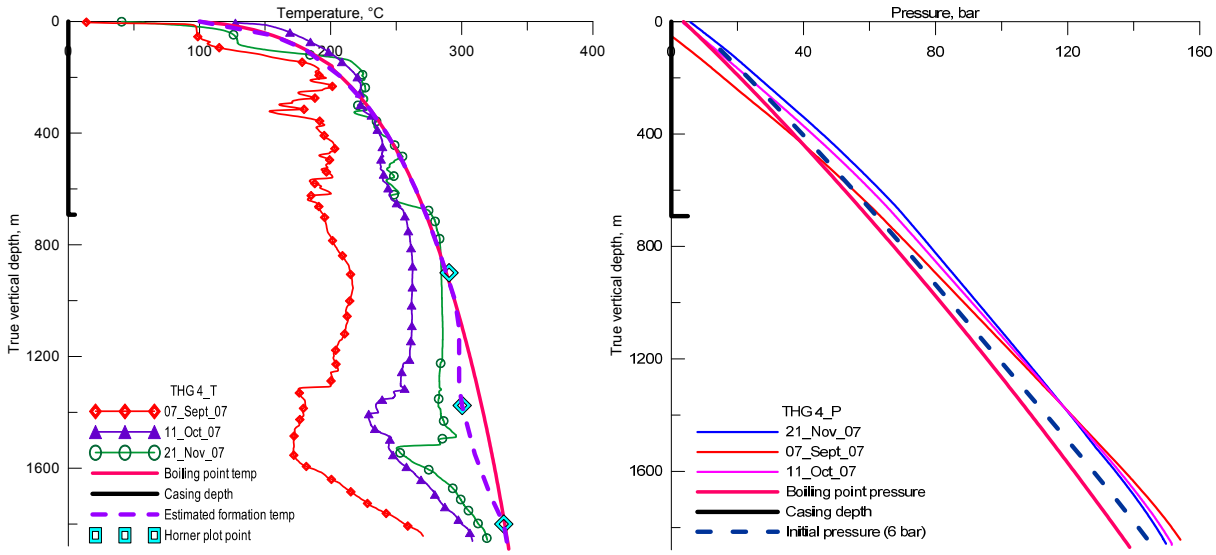

FIGURE 3: Well THG-4, estimated formation temperature (left) and initial pressure (right)